NUREG/CR-2951
SAND84-1838
R7
Printed April 1985

The D9 Experiment: Heat Removal From Stratified UO_2 Debris

C. A. Ottinger, G. W. Mitchell, R. J. Lipinski, J. E. Kelly

Prepared by
Sandia National Laboratories
Albuquerque, New Mexico 87185 and Livermore, California 94550
for the United States Department of Energy
under Contract DE-AC04-76DP00789

Prepared for
U. S. NUCLEAR REGULATORY COMMISSION

Available from

Superintendent of Documents
U.S. Government Printing Office
Post Office Box 37082
Washington, D.C. 20013-7982

and

National Technical Information Service
Springfield, VA 22161

NUREG/CR-2951
SAND84-1838
R7

THE D9 EXPERIMENT: HEAT REMOVAL FROM STRATIFIED UO_2 DEBRIS*

C. A. Ottinger
G. W. Mitchell
R. J. Lipinski
J. E. Kelly

Printed: April 1985

Sandia National Laboratories
Albuquerque, NM 87185
Operated by
Sandia Corporation
for the
U.S. Department of Energy

Prepared for
Division of Accident Evaluation
Office of Nuclear Regulatory Research
U.S. Nuclear Regulatory Commission
Washington, DC 20555
Under Memorandum of Understanding DOE 40-550-75
NRC FIN No. A1181

*This work was supported by the U.S. Nuclear Regulatory Commission, Euratom Joint Research Center, and the Japanese Power Reactor and Nuclear Fuel Development Corporation.

ABSTRACT

The D9 experiment investigated the coolability of a shallow (77 mm), stratified urania bed in sodium. The bed was fission heated in the Annular Core Research Reactor (ACRR) at Sandia National Laboratories to simulate the effects of radioactive decay heating. It was the first stratified debris bed experiment to use an extended UO_2 particle size distribution (0.038 to 4.0 mm). Dryout occurred at powers ranging from 0.10 to 0.58 W/g, which was close to the incipient boiling power and before channels penetrated the subcooled zone in the bed, even with subcoolings as low as 80°C. Channel penetration was observed after dryout began, but the bed became only moderately more coolable. All these observations agree with current models.

Rapid increases in power to prototypic decay power levels yielded dry zone thicknesses similar to those expected from a very slow increase. Repeatable and reversible channel formation was observed during extended dryouts. A large superheat (90°C) flashing event increased the incipient dryout power from 0.2 to 4.4 W/g, presumably because it disrupted the bed stratification. However, superheat in excess of 30°C could not be achieved with a large power-step prototypic of heating in accident debris.

The D9 experiment provided significant new data on coolability of debris beds. Phenomenological information was derived for incipient dryout powers, bed channeling, extended dryouts, prototypic power steps, and superheat flashing. The incipient dryout powers were low, implying that such debris beds would not be coolable for significant times after the onset of an accident. These data are extremely valuable for validating the models used in assessing reactor safety. The current coolability model developed by Lipinski was able to predict accurately all of the incipient dryout, extended dryout, and channeling behavior. This good agreement and the fact that the model is physically based indicates that it may be used to assess coolability questions related to debris bed behavior under a variety of accident conditions.

CONTENTS

		Page
1.	INTRODUCTION	1
2.	EXPERIMENT DESIGN	3
	2.1 Experiment Description	3
	2.1.1 Experiment Section	3
	2.1.2 Instrumentation	9
	2.2 Debris Bed Characteristics	9
3.	EXPERIMENT OPERATION AND RESULTS	16
	3.1 Session 1	16
	3.1.1 Session 1 Bed Power Calibration Determination	16
	3.1.2 Session 1 Nonboiling Control Runs	17
	3.1.3 Bed State at the Start of Session 1	17
	3.1.4 Session 1 Incipient Dryout Measurements	20
	3.1.5 Session 1 Channel Formation	26
	3.1.6 Session 1 Flashing	27
	3.1.7 Bed State at the End of Session 1	27
	3.2 Session 2	28
	3.2.1 Bed State at the Start of Session 2	28
	3.2.2 Session 2 Large Power Step Tests	28
	3.2.3 Session 2 Dryout Measurements	37
	3.2.4 Session 2 Channel Formation	37
	3.2.5 Session 2 Flashing	37
	3.2.6 Bed State at the End of Session 2	40
	3.3 Session 3	40
	3.3.1 Session 3 Dryout and Channeling Investigations	40
	3.3.2 Session 3 Flashing	45
	3.3.3 Bed State at the End of Session 3	47
	3.4 Session 4	47
	3.4.1 Session 4 Dryout Measurements	48
	3.4.2 Session 4 Flashing	48
	3.4.3 Bed State at the End of Session 4	48
4.	POSTTEST X-RAYS	53
5.	SUMMARY	56
6.	REFERENCES	58

LIST OF FIGURES

Figure		Page
2-1	Experiment Assembly Installed in the ACRR	4
2-2	D9 Experiment Section	5
2-3	D9 Insulated Crucible	6
2-4	D9 Primary and Secondary Containment Assembly	8
2-5	D9 Bed and Sodium Instrumentation	10
2-6	D9 UO_2 Debris Bed Loading	12
2-7	X-ray of D9 Following Loading of UO_2 and Sodium	14
2-8	X-ray of D9 Following Loading of UO_2 and Sodium	15
3-1	Nonboiling Control Run Bed Temperatures	18
3-2	Session 1 Control Runs and Power Calibration	19
3-3	Session 1 Dryout Measurements	21
3-4	Session 1 Dryout and Channel Formation	22
3-5	Session 1 Incipient Dryout Measurements	25
3-6	Session 2 Power Steps	29
3-7	Session 2 Power Steps	31
3-8	Session 2 Power Steps	32
3-9	Session 2 Bed Response to Power Step (Power Step 4)	34
3-10	Session 2 Bed Response to Power Step (Power Step 10)	35
3-11	Session 2 Bed Response to Power Step (Power Step 14)	36
3-12	Sessions 2 and 3 Incipient Dryout Measurements	38
3-13	Transitory Dryout Measurements	39
3-14	Session 3 Power Steps	41
3-15	Session 3 Dryout and Channel Formation	42
3-16	Session 3 Flash and Subsequent Dryout	43
3-17	Session 3 Flash and Subsequent Dryout	44
3-18	Session 3 Zone Thickness Predictions and Measurements	46
3-19	Session 4 Search for Dryout	49
3-20	Session 4 Flashing	50
3-21	Session 4 Flashing	51
3-22	Superheat at Flashing	52
4-1	Posttest X-ray of D9	54
4-2	Posttest X-ray of D9	55

LIST OF TABLES

Table		Page
2-1	UO_2 Particles in D9 Debris Bed	13
3-1	Incipient Dryout Powers in D9.	23
3-2	Large Power-Step Tests	30

1. INTRODUCTION

The Debris Bed Experiment Program at Sandia National Laboratories is jointly sponsored by the USNRC, the Joint Research Center Ispra (EURATOM), and the Power Reactor and Nuclear Fuel Development Corporation (PNC) of Japan. The program investigates the coolability of UO_2 particulate debris which can form following a severe core-disruption accident in a sodium-cooled nuclear reactor. The debris is heated by radioactive decay which is simulated in these experiments by fission heating fully enriched UO_2 particulate using the Annular Core Research Reactor (ACRR) at Sandia National Laboratories. Sodium, present in the reactor accident, is also contained in the experiment as a coolant.

The Debris Bed Experiments were designed to investigate the important factors which can affect the coolability of debris beds and provide the data base for use in model development and verification. Stratification is one such factor that affects the coolability of debris beds. Stratification can occur in many accident scenarios. For example, if the debris settles through an overlying pool of sodium prior to forming the bed, the large particles would sink faster than small ones resulting in a debris bed with large particles on the bottom with decreasing particle sizes toward the top of the bed.

The D9 experiment is the ninth in the series of twelve debris bed experiments and investigated the coolability of a shallow, stratified urania debris bed with an extended UO_2 particle size distribution in sodium. The D9 experiment was the third D-series experiment to study the effects of stratification on coolability and dryout power. In previous stratified debris bed experiments (D6 and D7), a particle size range of 0.1 mm to 1.0 mm was used. D9 was the first of the stratified experiments to use an extended particle size distribution from 0.038 mm to 4.0 mm to better simulate the size ranges of fragments observed in the quenching of UO_2 by sodium.[1] The D9 experiment had the same bed height (77 mm) as the previous stratified bed experiment (D7) but was designed to have an even lower range of sodium subcooling (as low as 70°C) than the D7 experiment (130°C minimum) to aid in the investigation of channeling.

The UO_2 particulate was held in a crucible with insulated sides and bottom to simulate a portion of a larger debris bed found in accident scenarios. This also allowed for easier analysis and subsequent modeling efforts which are necessary to evaluate debris beds under conditions other than those few examined experimentally.

The sodium pool above the debris bed in every D-series experiment is subcooled below the sodium saturation temperature. Subcooled sodium pools are expected in many accident scenarios. The subcooling in the D9 experiment was varied over a wide range (70° to 415°C) to study its effect on dryout power.

The D9 experiment was conducted in October 1982 with approximately 74 hours of nuclear heating and many more hours of heatups and shutdowns. Subcooling effects, dryout, post-dryout behavior, channeling, large power steps, and liquid superheat flashing were studied over the course of the experiment. The experiment apparatus is described first, followed by the operation and observations of the experiment.

2. EXPERIMENT DESIGN

2.1 Experiment Description

The D9 experiment hardware consisted of an experiment section specific to this test and an access section and closed helium cooling loop which are common to other debris bed experiments. A once-through nitrogen cooling system was also used during the last session of the experiment in place of the helium loop because of a failure in the helium system. The access section provided the piping for helium and instrumentation cables. The experiment section and access section were connected and placed in the central cavity of the Annular Core Research Reactor at Sandia National Laboratories (Figure 2-1). The access section helium piping was connected to the helium cooling loop via an overhead through. All instrumentation was then connected to the data acquisition system.

2.1.1 Experiment Section

The experiment section is shown in Figure 2-2. The UO_2 particulate was held in a double-walled insulated crucible suspended from the primary containment cover plate. The primary containment assembly served as the radiological containment as well as the sodium containment. An evacuated expansion tank, which served to reduce the cover gas pressure and extend the subcooling range, was opened to the primary containment remotely during the experiment. A secondary radiological containment assembly surrounded the primary. A helium cooling system surrounded the secondary containment and removed heat from the bulk sodium above the debris bed. Insulation was placed around the helium system to reduce heat losses from the experiment.

A double-walled insulated crucible was used to hold the UO_2 debris bed (Figure 2-3). The inner wall of the crucible was machined from Inconel 617 as a single unit. The outer wall and small pinch-off tube were fabricated as a single unit from stainless steel 321. The insulation between the two cylinders was Min-K 2000. An extensive procedure was adopted to prevent out-gassing of the insulation during the experiment operation which would lead to pressurization of the sealed crucible. First the insulation was baked out in a vacuum furnace at about 10^{-5} torr by heating from room temperature to 650°C over a period of 5 hr and then maintaining 650°C for approximately 2 hr. After the insulation was placed between the walls of the crucible, a single electron beam weld was made at the top of the outer cylinder to the flange of the inner cylinder. Then, the assembled crucible containing the insulation was baked out again while evacuating through the small tube. The crucible and insulation were heated from room temperature to 700°C over a

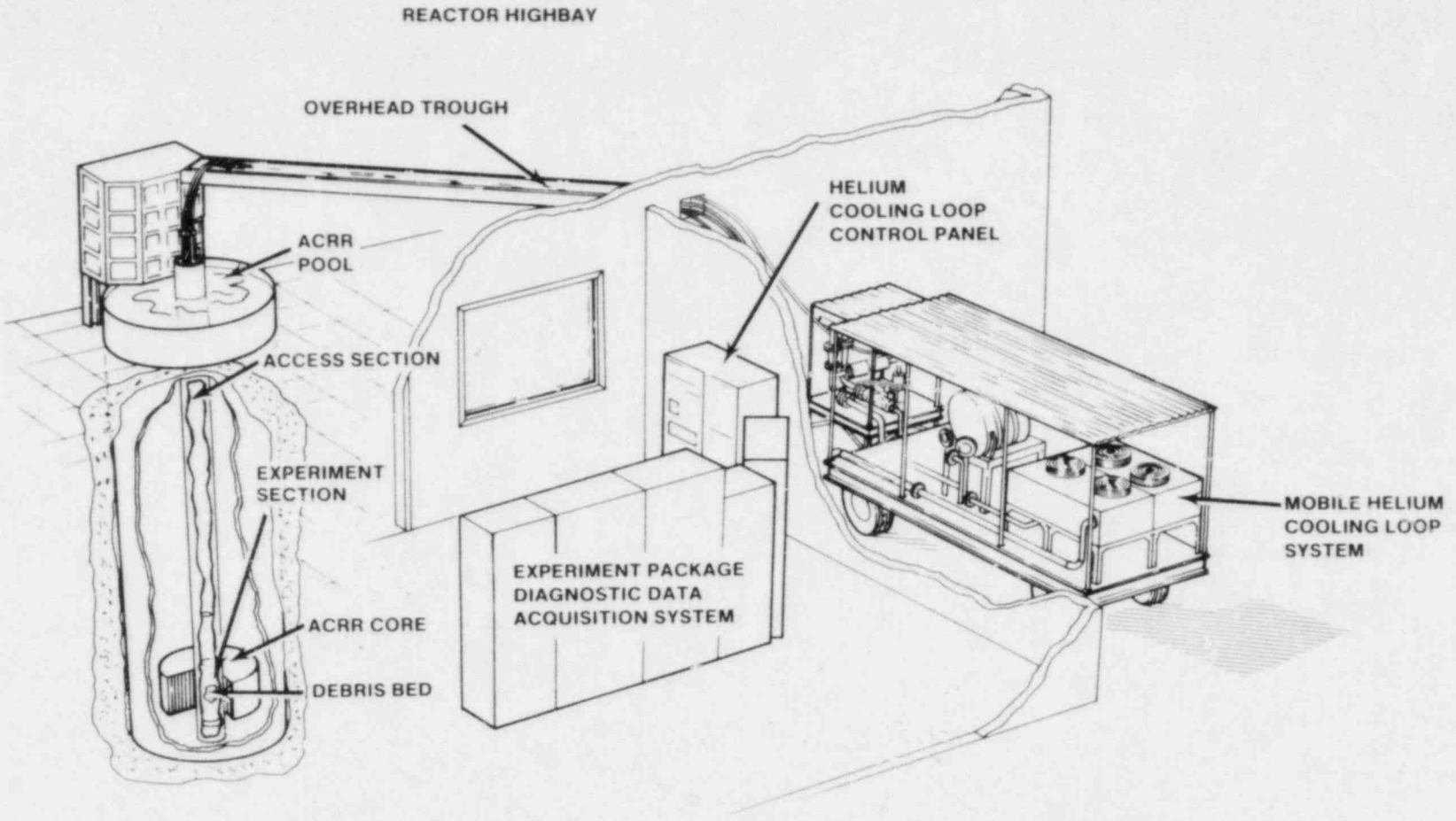

Figure 2-1. Experiment Assembly Installed in the ACRR

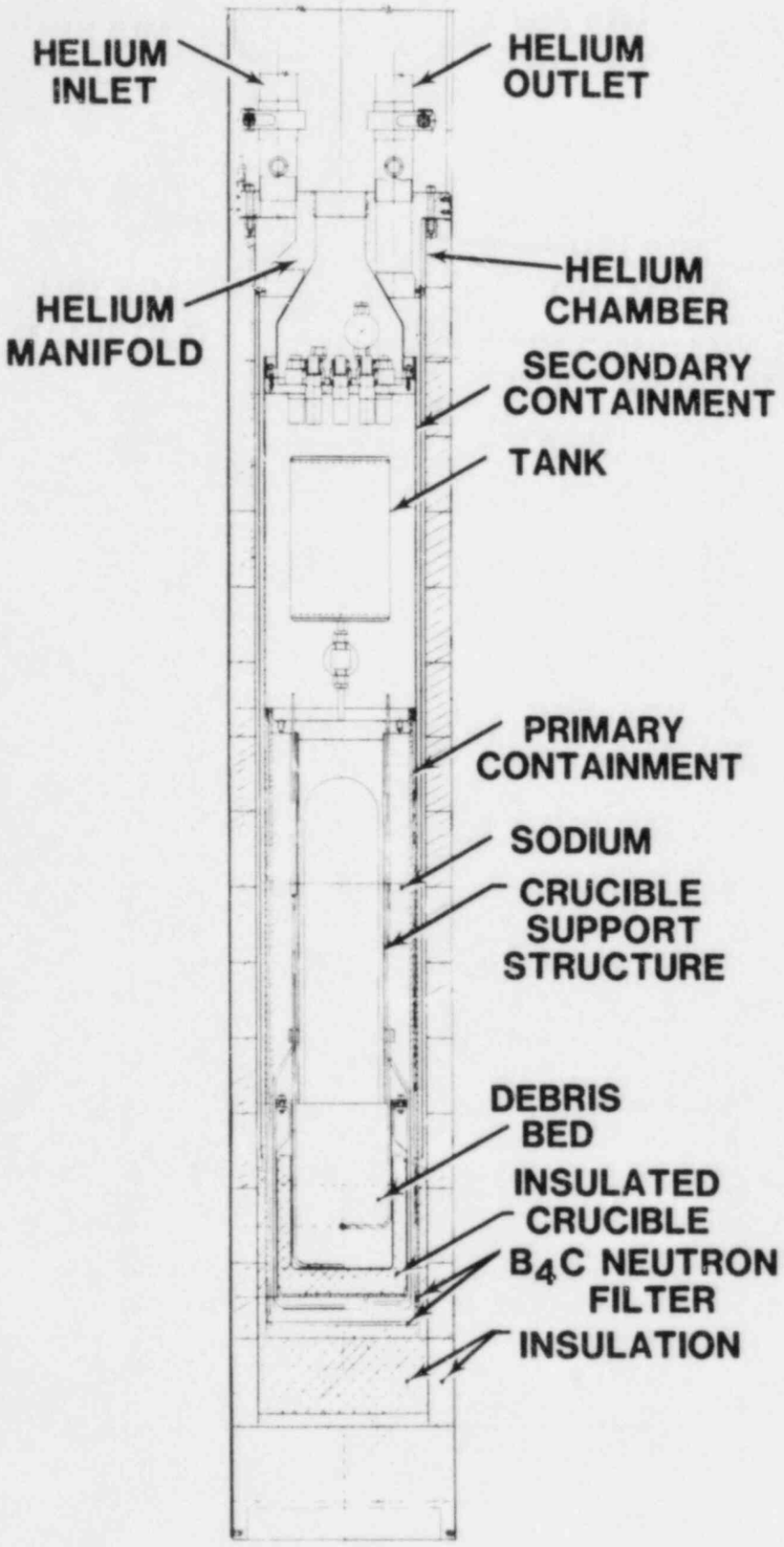

Figure 2-2. D9 Experiment Section

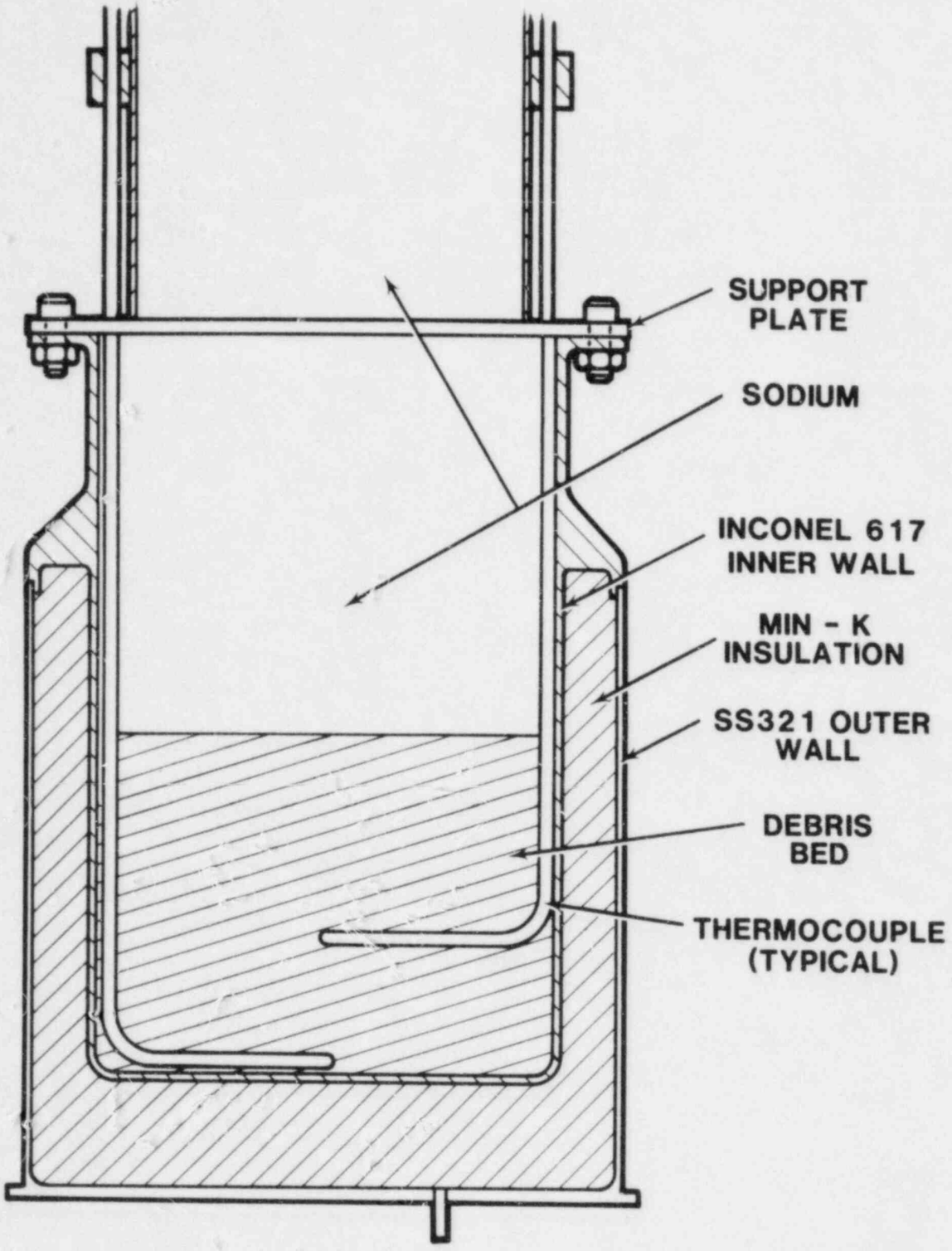

Figure 2-3. D9 Insulated Crucible

period of 4.5 hr and held at a maximum temperature of 700°C for 11 hr. The insulation was left under vacuum while the small tube was pinched off and sealed with an electron beam weld. To insure that the bake-out process had been adequate, the sealed crucible was again heated to 700°C over a period of 5 hr and held for 45 min prior to a final helium leak check of the integrity of the crucible walls.

The primary containment consisted of a 321 stainless steel cylinder and a 316 stainless steel cover plate which threaded into the cylinder at the top and was sealed with a weld (Figure 2-4). All containment penetrations were made through the cover plate. The crucible was suspended from a central support column welded to the cover plate. Side openings in the support column allowed for loading of UO_2 into the crucible. Prior to attachment of the crucible, Inconel-sheathed K-type thermocouples were fed through the cover plate, positioned, and secured on the solid sides of the support column by brackets. The thermocouples were then brazed into the cover plate using a high nickel content braze (Nicrobraze 125). Following loading of the debris bed into the crucible, the cylinder was threaded onto the cover plate and sealed with a weld.

An expansion tank, made of 321 stainless steel, was connected to the primary containment through a one-time use valve. An orifice disk was placed in line with the valve to limit the rate of change of pressure between the tank and the primary containment. After the tank was evacuated, the valve was closed. The valve was opened remotely during the experiment using an electric heater which melted a silver braze joint (T_{melt} = 730°C) in the valve knob.

Electrical heaters were located in the bulk sodium above the debris bed and served to melt the sodium at the start of the experiment. The heaters also helped to achieve high bulk sodium temperatures when the bed was at low powers. These heaters were operational during the first 13 hr of the experiment.

A secondary containment surrounded the primary containment and served as a backup radiological containment in the event of leakage from the primary containment. The 321 stainless steel secondary containment consisted of a cover plate welded into the top of a cylinder. Again, all penetrations were made through the cover plate. Electrical connections for the thermocouples and heaters were made to feedthroughs prior to installation and welding of the cover plate to the cylinder. The feedthroughs contain chromel and alumel wires with glass-to-metal hermetic seals. The feedthroughs were sealed to the cover plate by pulling the tapered body of each feedthrough into holes in the cover plate, making a metal-to-metal seal.

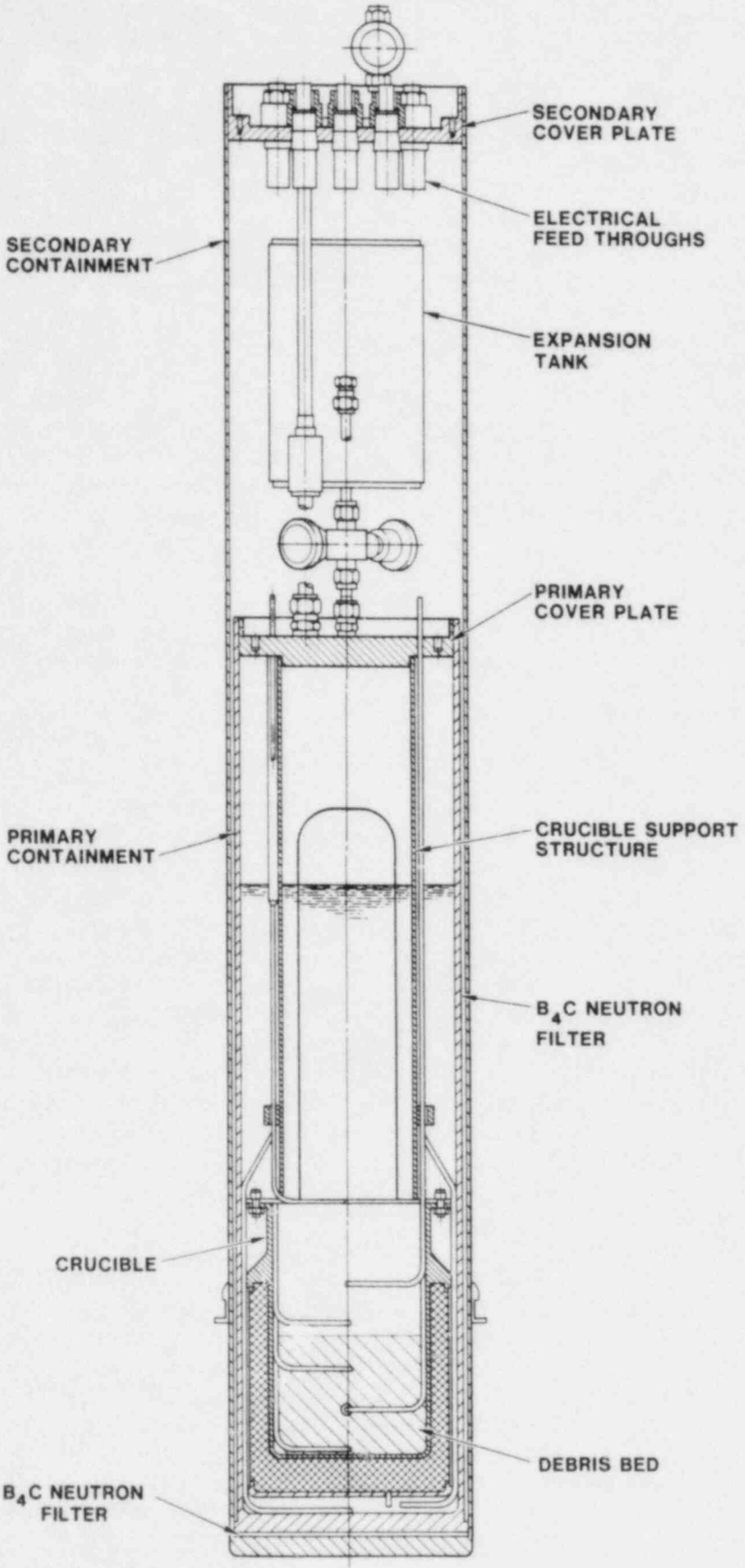

Figure 2-4. D9 Primary and Secondary Containment Assembly

Powered B_4C was placed between the sides of the primary and secondary containment cylinders to harden the neutron spectrum and flatten the power profile within the debris bed. The powder was packed to a density of approximately 1.2 g/cm^3. A plate of dense B_4C was placed between the bottoms of the containment cylinders. Neutronic calculations were performed for the experiment configuration prior to the experiment operation. These calculations indicate that the B_4C filters produce a radial peak to average power in the debris bed of 1.17 and an axial peak to average power of 1.11.[2]

A stainless steel helium chamber surrounded the containment cylinders. A manifold above the containment cylinders directed helium flow to the containment cylinders and also provided a central port to allow the passage of all instrumentation and electrical wires. The helium flow provides cooling of the sodium pool above the debris bed.

2.1.2 Instrumentation

Inconel sheathed K-type thermocouples provided the primary instrumentation for the D9 experiment. Both single and multijunction thermocouples were used in the experiment. The thermocouples were baked out at 500°C under vacuum for 5 hours prior to installation in the experiment. Sixteen thermocouple junctions were located in the bed at axial locations of 1.5 (B0x), 10 (B1x), 20 (B2x), 35 (B3x), 50 (B4), and 65 (B5) mm with respect to the bottom of the bed. Three thermocouples (S1, S2, S3) were located in the sodium above the bed to monitor bulk sodium temperatures. Five (C1, C2, C3x) were located in the sodium surrounding the crucible to monitor radial and downward heat losses from the bed and to monitor containment boundary temperatures. Locations of these thermocouples are shown in Figure 2-5. Eighteen thermocouple junctions were located in the insulation around the helium chamber and next to the outer shell to monitor heat losses from the experiment. Eleven more thermocouples were located elsewhere in the package to monitor other component temperatures.

The thermocouple data were scanned at 5-second intervals for real time display and for storage on an HP-1000 system. The data were also sampled at 1-second intervals by an analog-to-digital converter and stored on a disk by an HP-9845B computer.

2.2 Debris Bed Characteristics

The debris bed consisted of 3500 g of UO_2 particulate with an extended size distribution (particle size ranges from 0.038 mm to 4.0 mm). The particles had been separated into 14 groups and were loaded into the crucible one group at a

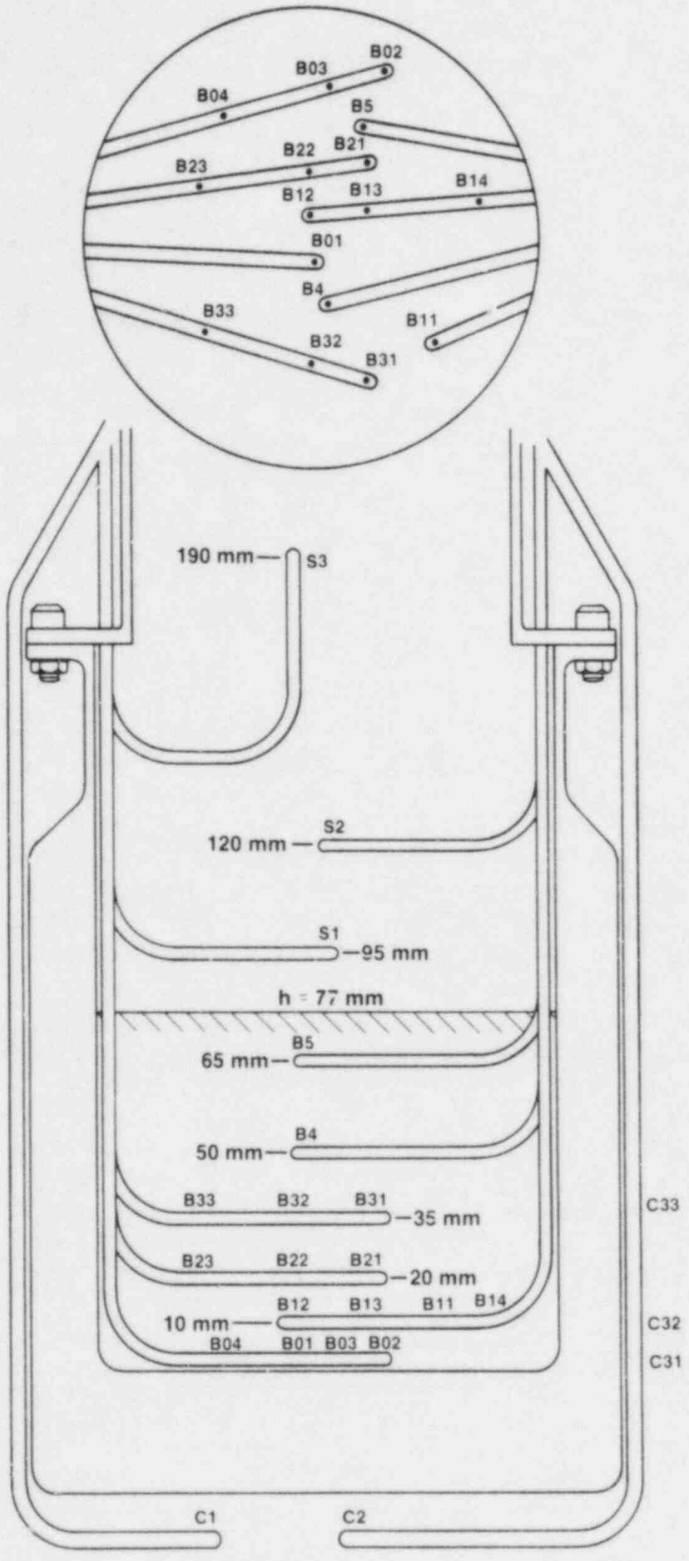

Figure 2-5. D9 Bed and Sodium Instrumentation

time with the largest particles on the bottom. The height to the top of each layer was measured after it was loaded (Figure 2-6). Each layer was level within 2 to 3 mm. The final measured height of the bed was 74 to 77 mm. The weight and size of each group are listed in Table 2-1. The UO_2 was then baked out under vacuum for 6 hr at 300°C to 390°C. The final bed height was determined from x-rays (Figures 2-7 and 2-8) taken following sodium filling and ranged from 80 mm down to 70 mm (where the sodium entered the bed during filling), with an average height of 77 mm. The average bed porosity was calculated to be 43.5 percent. The walls of the crucible extend 8.6 to 9.6 cm above the top of the bed.

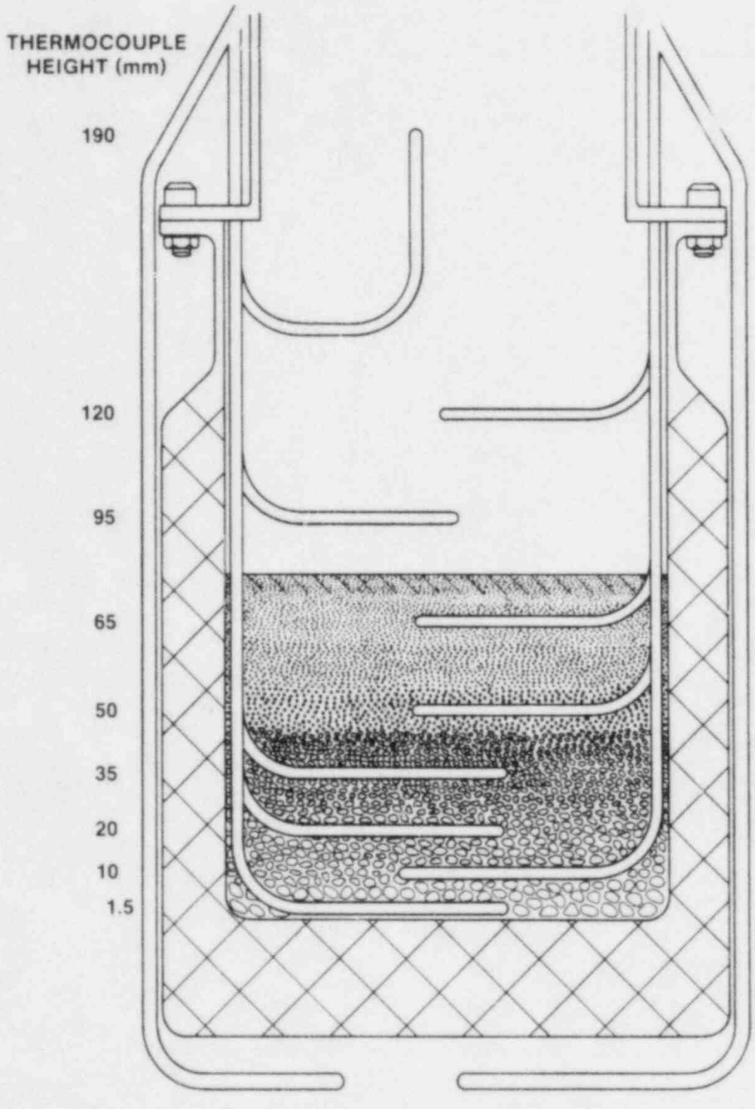

PARTICLE SIZE RANGE (microns)	HEIGHT TO TOP OF LAYER (mm)
38-45	75
45-63	72
63-90	69
90-125	65
125-180	58
180-250	53
250-355	44
355-500	37
500-710	29
710-1000	21
1000-1400	16
1400-2000	11
2000-2800	8
2800-4000	3

Figure 2-6. D9 UO_2 Debris Bed Loading

Table 2-1

UO_2 Particles in D9 Debris Bed

Particle Size Range (μm)	Mass of UO_2 (g)	Height to Top of Layer (mm)	Layer Thickness (mm)
2800-4000	126	3	3
2000-2800	165	8	5
1400-2000	228	11	3
1000-1400	273	16	5
710-1000	322	21	5
500-710	364	29	8
355-500	374	37	8
250-355	378	44	7
180-250	326	53	9
125-180	318	58	5
90-125	238	65	7
63-90	199	69	4
45-63	133	72	3
38-45	56	75	3

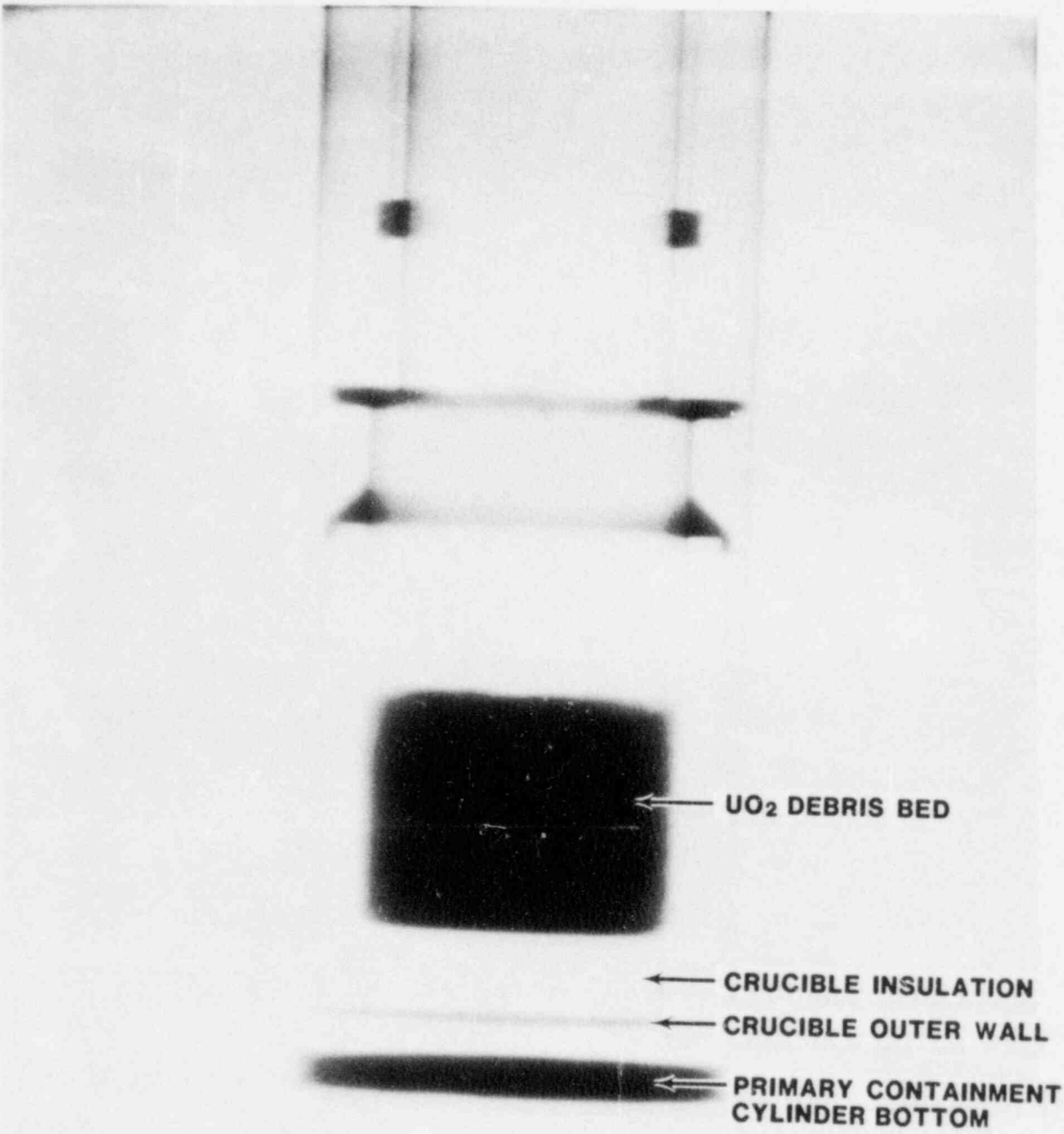

Figure 2-7. X-ray of D9 Following Loading of UO_2 and Sodium

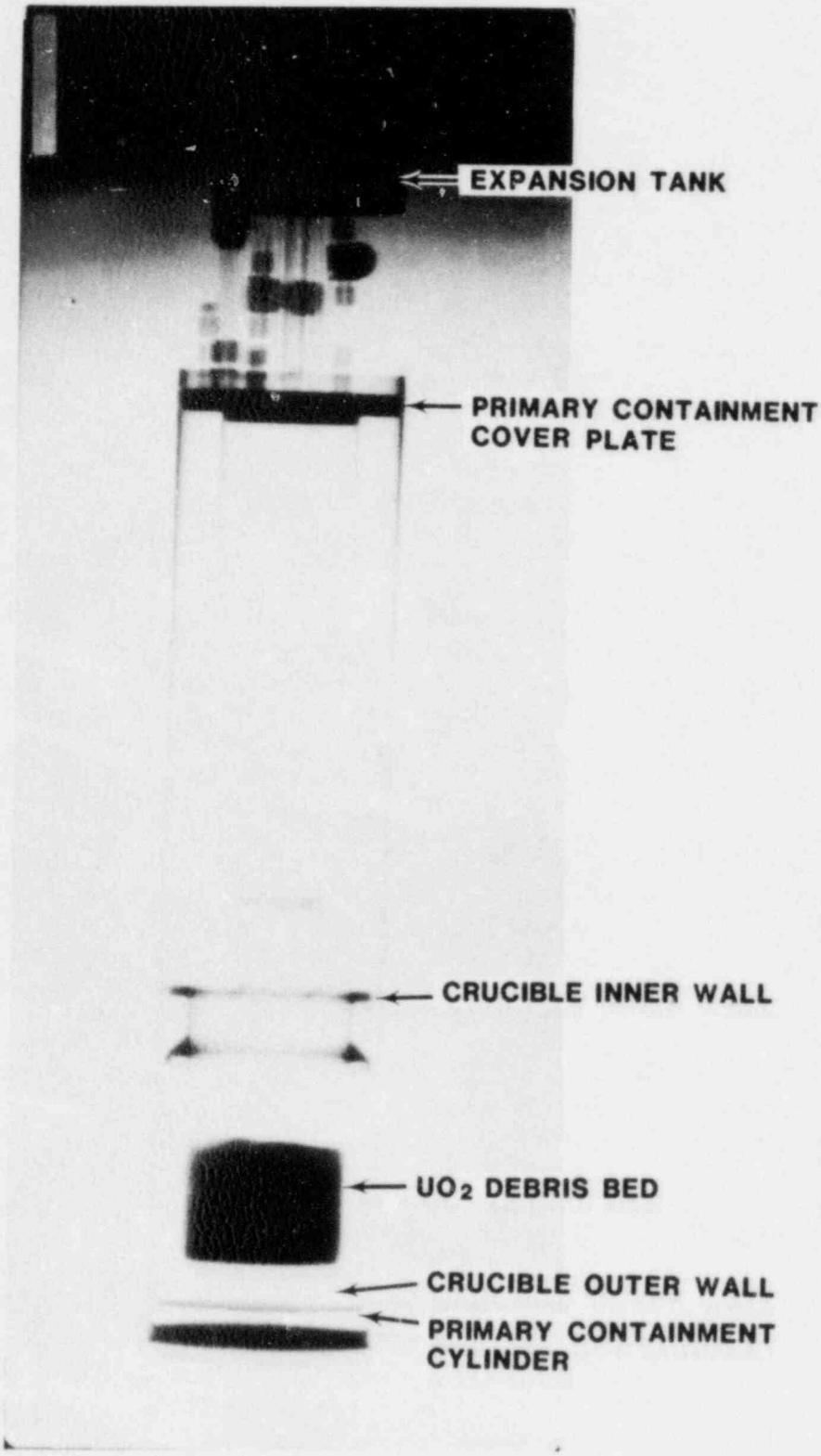

Figure 2-8. X-ray of D9 Following Loading of UO_2 and Sodium

3. EXPERIMENT OPERATION AND RESULTS

The experiment was conducted in four sessions over the period October 17-27, 1982 with approximately 74 hours of nuclear heating and 30 dryout investigations. The first session, conducted October 17-18, investigated incipient dryout as a function of sodium subcooling. Subcoolings as low as 70°C were achieved after the evacuated expansion tank was opened. Dryout occurred near incipient boiling, with incipient dryout powers of 0.10 to 0.46 W/g. The second session, conducted October 19, investigated the effect of large rapid power steps (up to 2.5 W/g) on the dryout powers. These step changes had minimal effect on the incipient dryout powers. The third session, conducted October 21-22, investigated extended dryouts to a maximum temperature of 1150°C and superheat flashing effects. Repeatable channel formation, which decreased the dry zone thickness, was observed. After prolonged boiling, a large superheat flashing event (approximately 90°C) was triggered. Following this event, the dryout power was 4.4 $\pm$ 0.6 W/g. The fourth session, conducted October 26-27, investigated superheat phenomena. Superheat flashing was achieved following boiling in the bed. Large power steps produced only small (approximately 20°C) superheat flashes.

3.1 Session 1

The first session investigated the incipient dryout powers and channeling behavior of stratified debris beds. As in all sessions, calibration and control runs consisting of steady-state operation at low power were made first in order to define the bed power and geometry. After these were completed, incipient dryout measurements were made for a wide range of subcoolings with the dryout powers remaining quite low (<0.46 W/g). Following the dryout study, the bed was heated rapidly using relatively small power steps. The rapid heating, which simulates the heating of an actual debris bed upon formation, caused channels to form, but dryout still occurred at low power.

3.1.1 Session 1 Bed Power Calibration Determination

The specific power (W/g UO_2) of the fuel relative to the ACRR reactor power was determined by the heatup rate of the bed in response to a step increase in power. Eleven such power calibrations were made during the conduct of the experiment (sometimes in conjunction with a large power-step test), always starting from a near steady-state nonboiling condition. The initial calibration test resulted in a coupling of 2.50 W/g UO_2/MW_{ACRR}. This value remained constant throughout the experiment.

3.1.2 Session 1 Nonboiling Control Runs

The state of the bed can be partly determined by comparing the bed temperatures with expected temperatures based on conductive heat flow. The temperatures from the control runs made at the start and end of each session are shown in Figure 3-1. The purpose of the control runs is to determine if changes had occurred in the bed as a result of a particular set of operations. Shown on the graph are the thermocouple readings from the bottom of the bed (0 at 1.5 mm) to the top of the bed (5 at 65.0 mm). On the left hand ordinate, the calculated temperatures at the thermocouple locations based on Kampf-Karsten's thermal conduction are shown. The most significant changes occurred in the bed during Session 1 and Session 3.

During Session 1 the bed was boiled for some time and channels were also formed. This modified the bed slightly such that the bed was cooler (better heat transfer) than at the start of Session 1. The bed was relatively unchanged during Session 2 but was changed significantly in Session 3 by the superheat flashing event. This disrupted the stratification in the bed and ejected debris out of the crucible. This is indicated by the 65 mm (B5) thermocouple which was then reading the sodium saturation temperature. The runs shown were all made with 300°C bulk sodium and 0.250 W/g-UO_2 (except for the end of Session 3 which was with 0.500 W/g-UO_2 and which has been normalized to 0.250 W/g-UO_2), allowing a more direct comparison of the data.

3.1.3 Bed State at the Start of Session 1

Two control runs were made near the start of Session 1 (Figure 3-2 at 11:25-11:45 and 12:50-12:58). The first run showed that, while the temperatures in the top of the bed were as predicted, the temperatures in the bottom of the bed were higher than predicted.[3] This discrepancy could be due to trapped gas or porosity variations. After heating the bed for a period to encourage wetting and gas release, the second control run was made and resulted in a slight decline in temperatures. This decline may be evidence of gas release. The measured temperature difference through the bed was 152°C after the power run for wetting. The calculated value was 118°C or 22 percent lower than measured. Part of this difference is due to errors in power level, coupling factor, and thermocouple location. However, it is evident that some additional resistance remained in the bed or the conductivity was slightly lower than predicted by Kampf-Karsten.

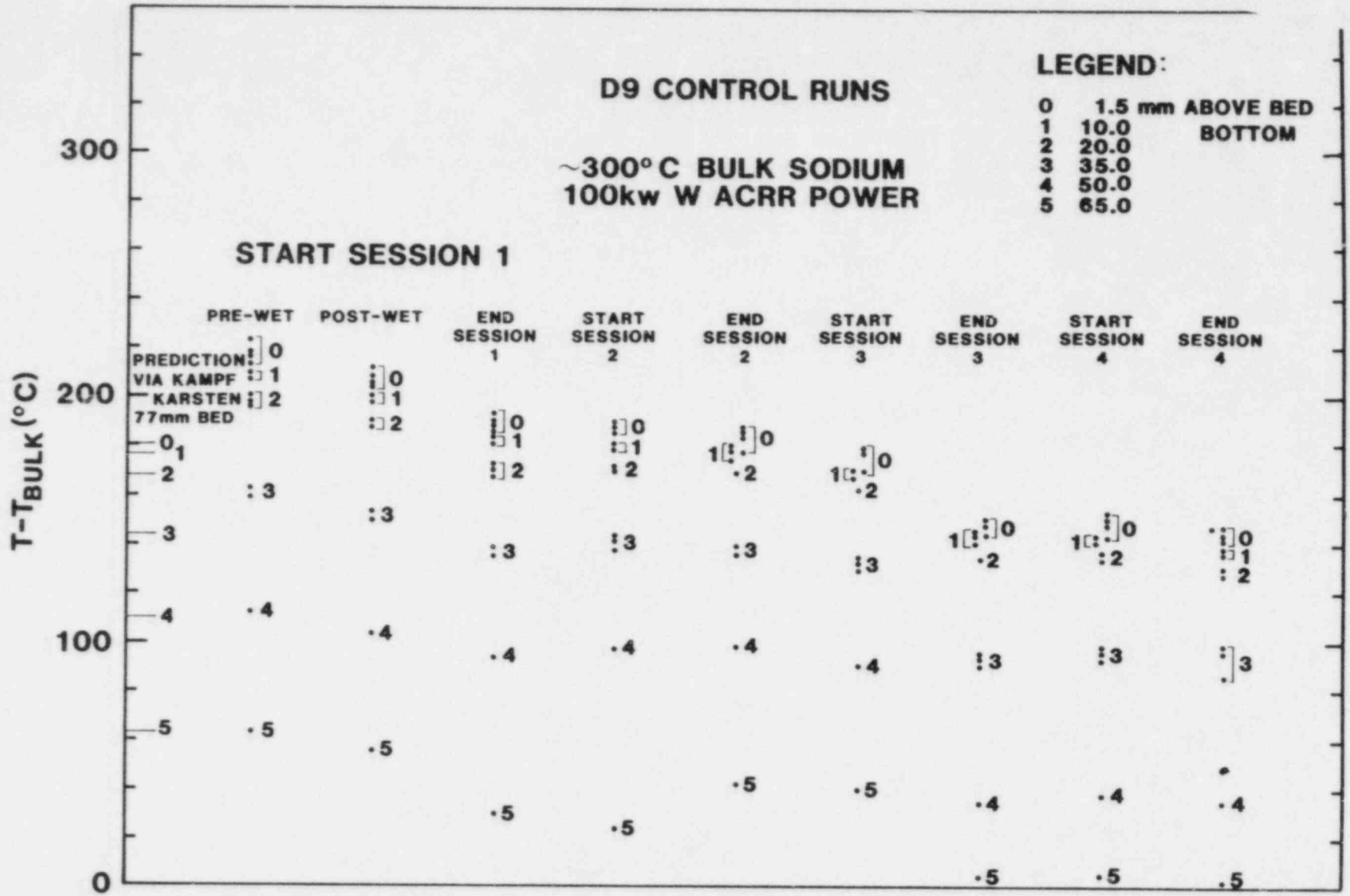

Figure 3-1. Nonboiling Control Run Bed Temperatures

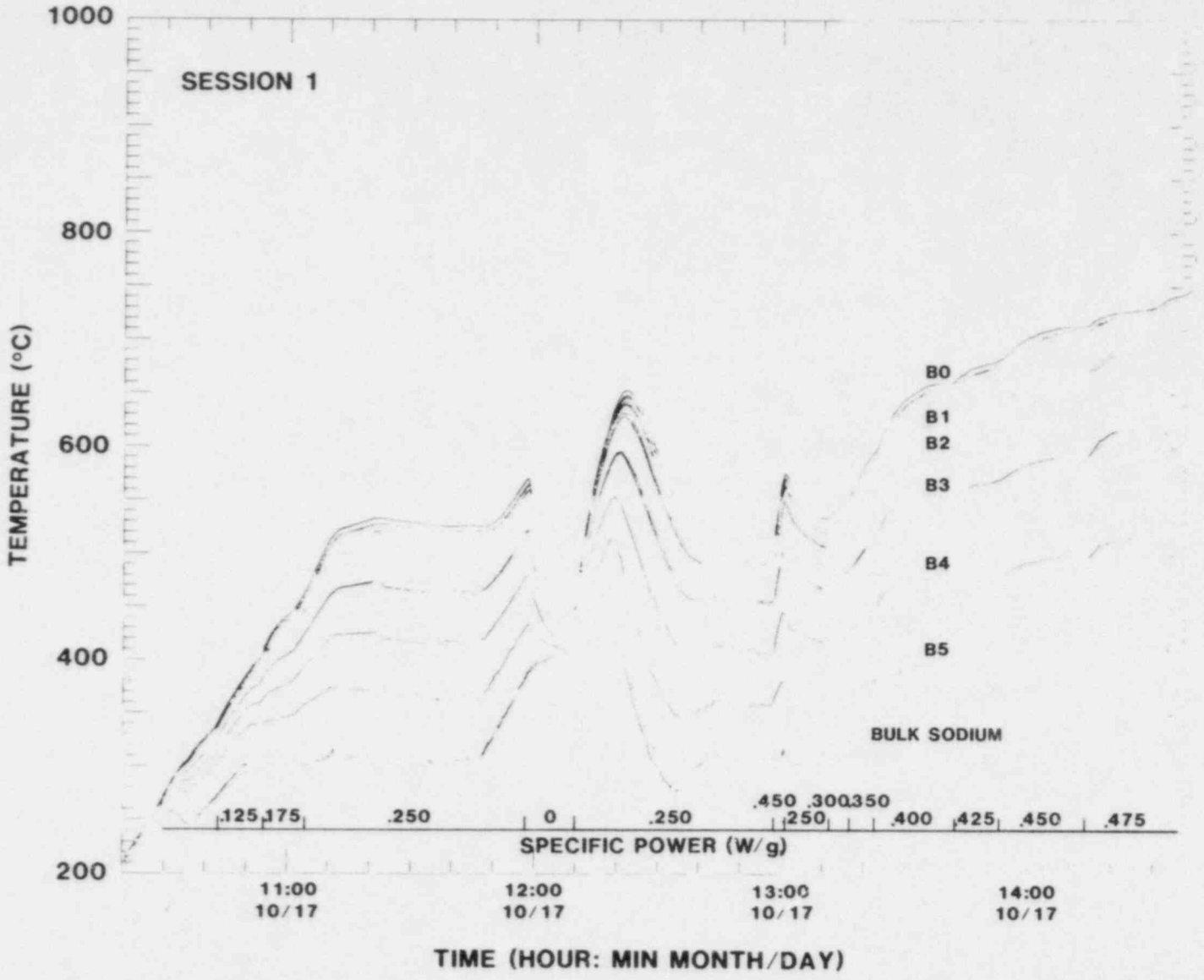

Figure 3-2. Session 1 Control Runs and Power Calibration

3.1.4 Session 1 Incipient Dryout Measurements

During the course of the experiment, 30 incipient dryout measurements were performed with 10 being made in the first session (Figures 3-2, 3-3, and 3-4). In most cases, the dryout power was determined by bracketing the incipient condition between two powers. That is, the power was held constant at a power below dryout and then increased in steps until dryout occurred; hence the dryout power lies between two power levels. Typically, the bed prior to dryout has a subcooled zone at the top of the bed with a boiling zone in the lower parts of the bed which is at the saturation temperature. As the power density is increased in the bed, a zone will "dryout" and the temperatures will increase above the saturation temperature. The saturation temperature is determined by the pressure in the vessel. Subsequent to a given dryout measurement, the power is lowered to reestablish boiling in the bed, the conditions are changed, e.g., sodium subcooling is decreased, and the process is repeated by increasing the power in steps.

In this session, however, with the boiling power so close to the incipient dryout power, the bed was not allowed to rewet. If the bed temperature was reduced below the boiling point, a superheat flash would be expected as the power was increased to the next incipient dryout power. This would risk disturbing the stratification in the bed before sufficient measurements could be made. Thus, in Figure 3-3, there is one incipient dryout point at 16:00 and the other dryout powers at different bulk sodium temperatures are inferred from changes in the bed temperatures. If the dry zone was going to rewet for a given power, that power was considered below the incipient dryout power.

The dryout powers for the entire experiment are given in Table 3-1 along with the bulk sodium and saturation temperatures and subcoolings. The uncertainty in the power is estimated to be about $\pm$ 0.02 W/g unless otherwise specified. Some dryouts (labeled T) were not stable, as will be described in the section on Session 2 results. Following dryout 5, the evacuated expansion tank connected to the primary containment was opened, as noted in Figure 3-3, causing a decrease in the package pressure. This decreased the saturation temperature and allowed a smaller subcooling while maintaining bulk sodium temperatures and containment temperatures within the experiment safety limitations. The impact of the pressure change on the bed structure was minimal. During depressurization, the boiling zone generated additional vapor because of the stored heat in the UO_2 particles as the saturation temperature decreased. This excess generation was equivalent to an increase in bed power of about 0.034 W/g (which is small compared to the fission power of 0.42 W/g at this time). The increase in bed height

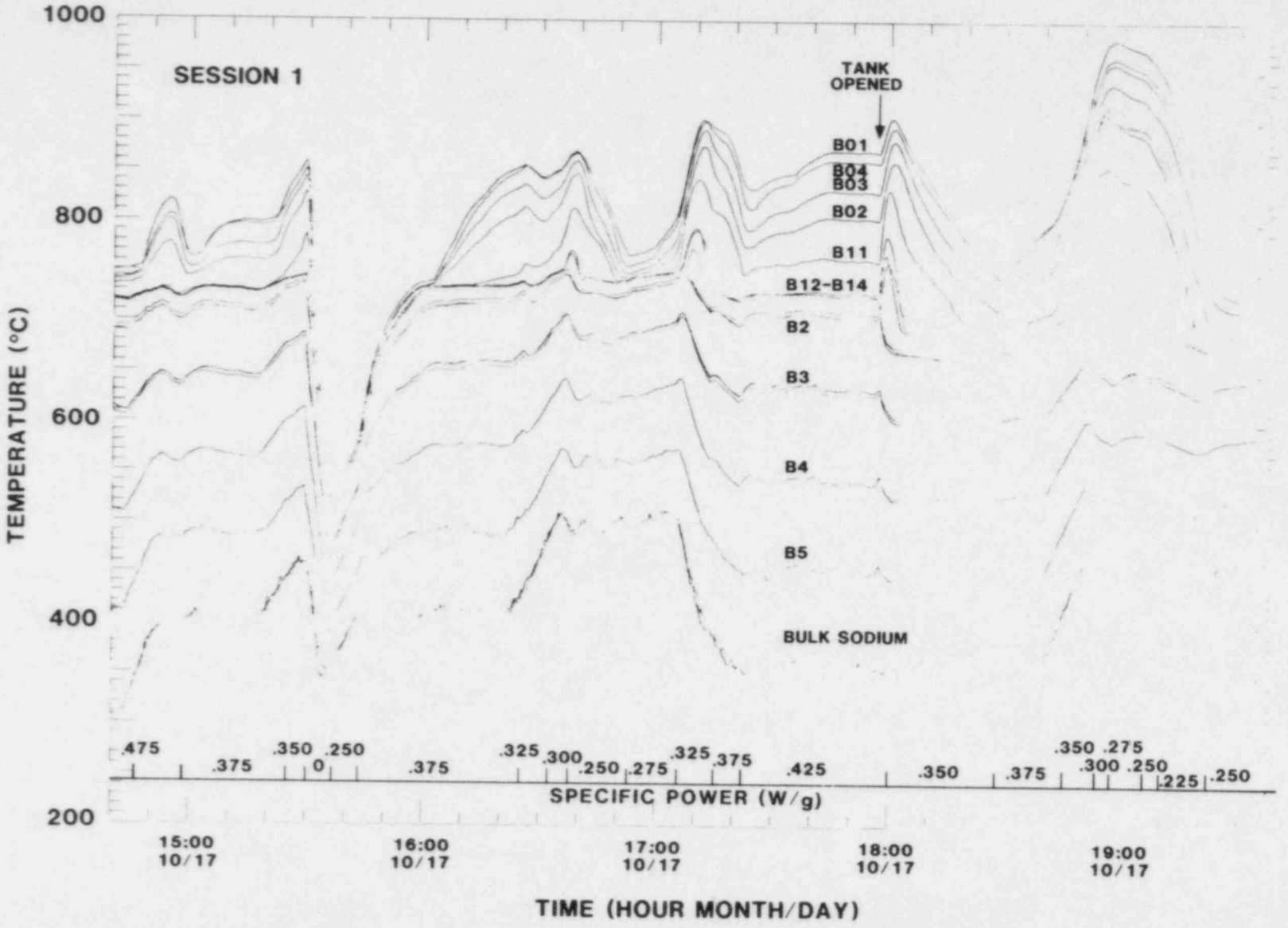

Figure 3-3. Session 1 Dryout Measurements

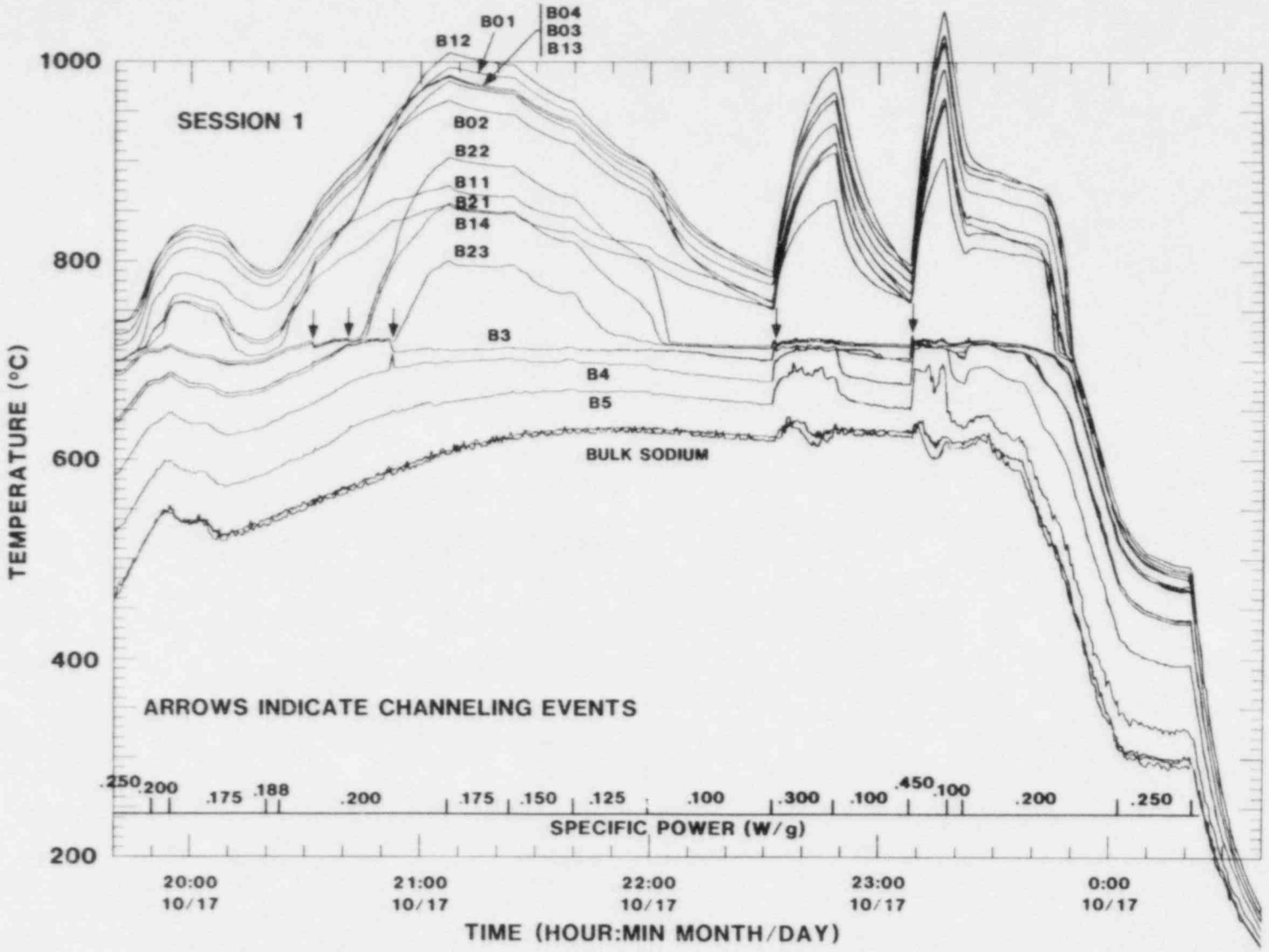

Figure 3-4. Session 1 Dryout and Channel Formation

Table 3-1

Incipient Dryout Powers in D9

Dryout Number	T_{bulk} (°C)	T_{Sat} (°C)	Subcooling (°C)	Power (W/g-UO_2)
Session 1:				
1	305	717	412	0.46
2	400	730	330	0.36
3	405	730	325	0.35
4	500	747	247	0.26
5	355	728	367	0.40
6	355	695	340	0.36
7	460	700	240	0.24
8	540	708	168	0.15
9	625	716	91	0.10
10	530	706	176	0.20
Session 2:				
11	375	698	323	0.43
12	370	692	322	0.44
13	460	700	240	0.35
14	550	702	152	0.29
15	650	720	70	0.50 T
16	605	714	109	0.38 T
17	645	720	75	0.38 T
18	640	719	79	0.20
19	640	720	80	0.23
20	370	700	330	0.50
21	500	700	200	0.36
22	560	710	150	1.0+0.1 T
23	305	690	385	0.58
Session 3:				
24	360	695	335	0.49
25	400	700	300	0.44
26	552	708	156	0.21
27	548	708	162	0.38
28	550	708	158	0.24
29	560	709	149	0.30
30	660	720	60	4.4+0.6

due to the increased vapor flow was estimated to be 2 mm or less.

The dryout points for Session 1 are plotted in Figure 3-5. Also shown are the predicted incipient boiling powers and dryout powers using the series conduction model and the one-dimensional dryout model described in Reference 4. The data from Session 1 (points 1 to 10) are very consistent and reproducible, and indicate that the measured dryout power is consistently lower than predicted. The reason for this is that the pressure in the D9 experiment package was greater than that used in the pre-experiment calculations and also that there was still some increased thermal resistance in the bed as compared with Kampf-Karsten equations. The dryout predictions implicitly depend on the conduction calculations being correct. The one-dimensional boiling and dryout model[4] predicts that dryout will occur very close to incipient boiling[3] which is in good agreement with the data. The first dryout point in Session 1 occurred within 5 percent of the incipient boiling power.

The reason for the dryout to occur near the onset of boiling is the effect of capillary force in stratified beds. Capillary force tends to keep the liquid in the region with the smallest particles, impeding the downward flow of the liquid and causing dryout almost as soon as boiling begins.

It is important to note that because of the strong surface tension in sodium, not much stratification is required to induce low dryout powers. For example, the first dryout point occurred with the boiling zone extending only over the bottom 10 mm of the bed. Above that, heat was removed in the subcooled zone by conduction. The particle diameters in the boiling zone ranged from 4.0 to 1.4 mm (bottom to top). The particle diameters spanned a factor of three in size. (The average size of the layers spanned only a factor of two.) Yet this small amount of stratification was sufficient to induce a low dryout power.

The dryout power in D9 did not increase dramatically at very low subcoolings as it did in D4. Since the subcooled zone in D4 was thinner than in D9, it was postulated that channel penetration of the thinner subcooled zone at low subcoolings allowed the higher dryout power in D4.[5] In D9, dryout occurred before channel penetration at all subcoolings investigated (except for the last dryout, as will be described later). This was predicted by the one-dimensional model[4] and again is a consequence of stratification: the dryout power in a stratified bed is so close to the incipient boiling power that the subcooled zone is thick and channels cannot penetrate. Such behavior was also seen in D6 and D7.[6,7]

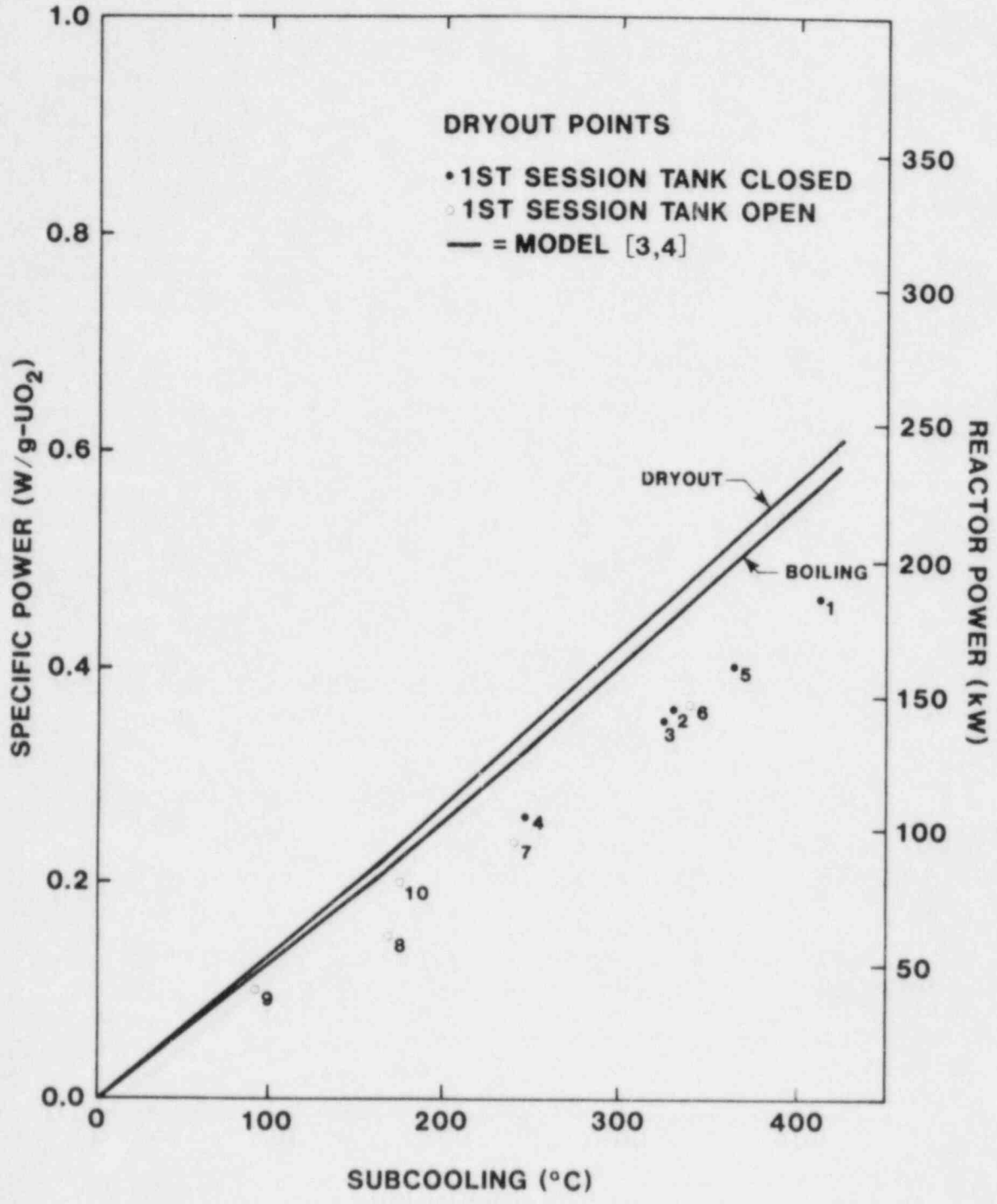

Figure 3-5. Session 1 Incipient Dryout Measurements

3.1.5 Session 1 Channel Formation

Detection of channel formation was one of the objectives of the experiment. The pretest predictions indicated that channeling would occur, but only after dryout. Consequently, channeling was not expected to provide an increase in the incipient dryout power. Furthermore, once the channels formed, they would not extend to the bottom of the bed and would only serve to decrease the size of the dry zone. The pretest predictions showed that with channeling the dry zone would be less than 20 mm thick, but certainly greater than 10 mm thick.

Experimentally, the occurrence of a channel was detected by a sudden reduction in the boiling temperature. This reduction occurred due to pressure relief in the lower region of the bed caused by the channel. Drops of about 7°C are predicted by the one-dimensional boiling model.[3,4] A superheat flashing event also produces a similar thermocouple response. The difference between the two is that channel formation must occur after boiling is initiated, while by definition a superheat flashing event must occur before boiling. Hence, by careful observation of the thermocouple readings, it is possible to differentiate between a channel formation and a superheat flashing event.

One must also be able to detect the onset of boiling in order to distinguish channeling from flashing. This is sometimes difficult because the saturation temperature is a function of vapor fraction and location in the bed because of varying capillary pressure. Such behavior was first noted in D5 and was also seen in D7.[8,7] However, one can detect the onset of boiling by noting when the temperature difference between two levels in the bed begins to decrease in response to a power increase, which results from the improved effective thermal conductivity from two-phase heat transfer.

Several sudden decreases in saturation temperature occurred in the first session (Figure 3-4 at 20:30, 20:40, and 20:53). The power was held constant and the bulk sodium temperature was allowed to increase in order to cause the subcooled zone in the bed to decrease. The 20-mm (B2x) level was definitely boiling during the first two decreases because the temperature remained nearly constant while the 35-mm (B3x) level temperature increased. Thus, the saturation temperature drops indicated channel formation or a bed loosening of some kind. These events occurred after dryout, as predicted, and at about the same subcooled zone thickness as predicted for channel penetration. However, they did not lead to a state of increased coolability. The dry zone temperature did not decrease and the 20-mm (B2x) level later became dry, indicating that the bed was still behaving as a packed bed. Thus, these events may have been the formation

of small internal channels that did not penetrate through the subcooled zone of the bed.

Following these events, two power steps were made (at 22:31-22:48 and at 23:08-23:17), and channeling was again observed (Figure 3-4). In this case, the 20-mm (B2x) level did not dry out, and the dry zone temperatures were cooler than they were previously with a lower power. This indicates that the bed was in a more coolable state and that channels may have penetrated the subcooled zone. Thus, the subcooled zone thickness required for channel penetration was slightly less than predicted, but the basic phenomenon was supported by these results. More direct support occurred in Session 3 and will be described later.

3.1.6 Session 1 Flashing

Superheat flashing was also investigated in the experiment. Flashing events result from the reactivation of deactivated nucleation sites. Before boiling can be initiated, the liquid temperature must exceed the saturation temperature in order to have vapor bubble growth. The degree to which the liquid temperature must exceed the saturation temperature is called superheat. The superheat needed to initiate boiling is inversely proportional to the radius of a nucleate bubble in a cavity. Current theory suggests that as boiling proceeds, trapped gas in the cavities escapes. If boiling ceases and the liquid becomes subcooled, the liquid may penetrate into the cavities deeper than before. The part of the cavity near the liquid will then wet, and the nucleate bubble for starting boiling will be smaller. Upon reheating, the amount of superheat needed for boiling will be greater.

While no direct study of flashing was made in the first session, one situation occurred which is related to the superheat flashing phenomenon. Shortly after the first dryout was attained, and after 75 minutes of boiling, the reactor scrammed (Figure 3-3 at 15:30) causing a loss of power and rapid temperature decrease. The bed became entirely subcooled and upon heating it was anticipated that a superheat flashing event would occur. Fortunately no such event occurred and the bed configuration was unaltered. Apparently, in this case, the bed had not boiled long enough to fully outgas the nucleation sites.

3.1.7 Bed State at the End of Session 1

During Session 1 the bed was boiled extensively and taken to elevated temperatures. During the control run at the end of Session 1 the temperatures through the bed, except at the top, were in fairly good agreement with the conduction model as compared to the bed at the start of Session 1. This infers that any additional trapped gas or nonwetting was

taken care of during Session 1. The channeling investigations may have opened up the top layers of the bed and provided increased cooling as indicated by B5. The extensive boiling also may have caused some bed settling which would have led to lower temperatures in the bed. A bed shortening or nonuniformity of about 4 mm would also account for the temperature at the 65-mm level. It is noted that the 65-mm level temperature increased during Session 2, indicating that the bed may have leveled or increased in height.

3.2 Session 2

Essentially all dryout investigations, both in the D-series experiments and elsewhere, have used small power increments so as to determine the incipient dryout power with precision. This also minimizes disturbances in the bed so that the bed state at dryout is better characterized. However, debris formed in an accident is at a decay power level around 1 to 3 W/g-UO_2, and the power decays very slowly. When the bed is formed by falling through liquid sodium, the particles are initially at low temperatures. Heatup calculations indicate that the bed could easily form before it had heated to the boiling point.[10] Thus, a more prototypic heating method than slow power increases would be a single power step to 1 W/g or more (starting with a partially heated bed). Fifteen such large power steps were performed in Session 2 to determine the behavior of the bed under these more prototypic conditions. Steps up to 1.4 W/g were taken with both boiling and subcooled initial conditions. The main result from these tests was that the dryout power was not significantly increased.

3.2.1 Bed State at the Start of Session 2

The nonboiling control run at the start of the second session (Figure 3-6 at 04:50-05:00) was essentially identical to the one at the end of the first session (Figure 3-1). This indicates that no major bed changes occurred during the freezing and reheating cycle between the first two sessions. Later control runs showed no significant changes during any of the freezing and reheating cycles.

3.2.2 Session 2 Large Power-Step Tests

All the power steps of D9 are summarized in Table 3-2 and the ones in Session 2 are shown in Figures 3-6, 3-7, and 3-8. Most of the power steps started with the bed below dryout, and some with the bed below boiling. Initial powers ranged from 0.05 to 0.45 W/g. Final powers ranged from 0.30 to 2.50 W/g. All step tests resulted in dryout, except for the last four, which either were deliberately terminated early or occurred after a significant bed change, which will be addressed in Section 3.3.2. In most of the tests the dry

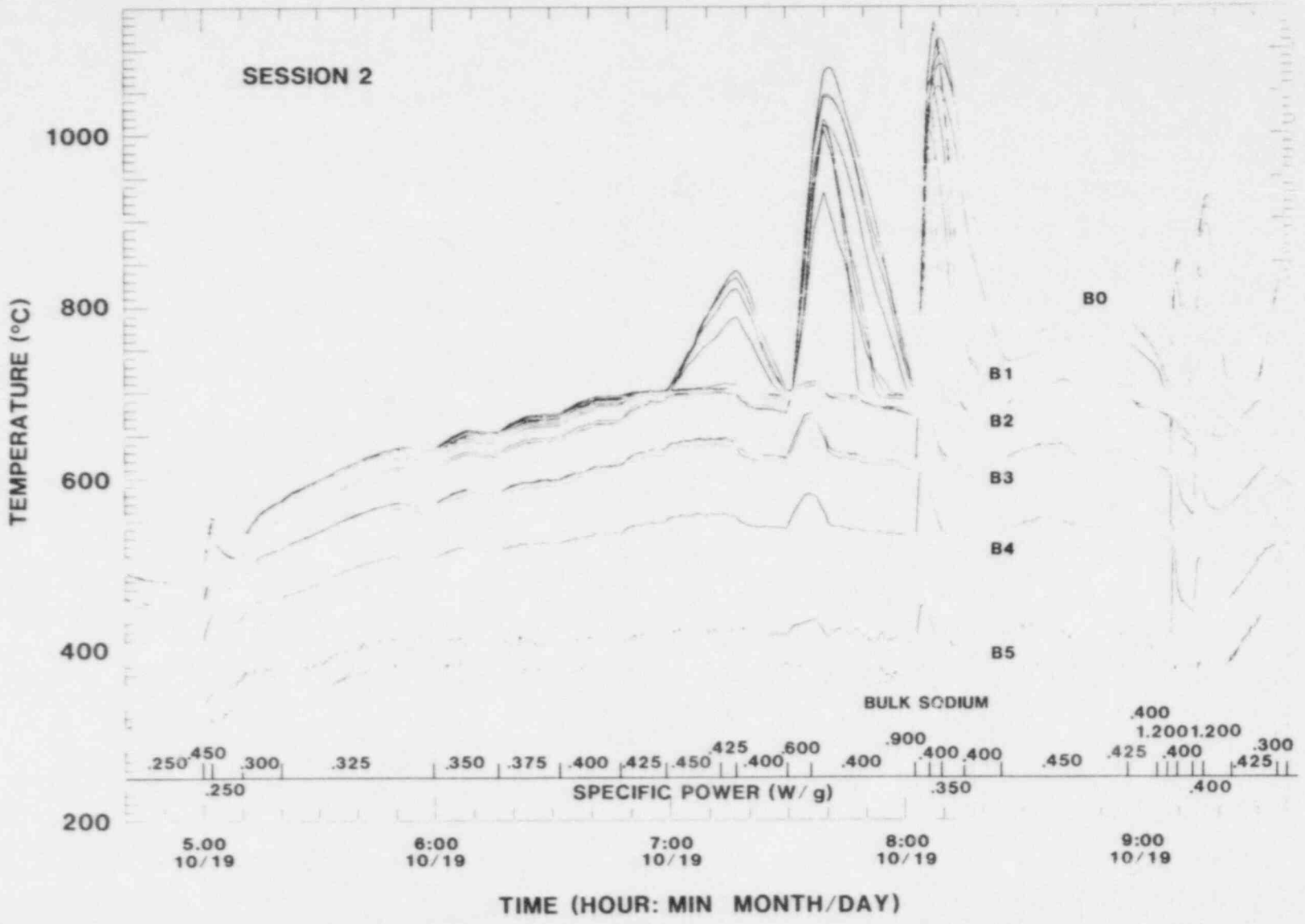

Figure 3-6. Session 2 Power Steps

Table 3-2

Large Power-Step Tests

Step Number	T_{bulk} (°C)	Initial T_{max} (°C)	Initial Power (W/g)	Final Power (W/g)	20-mm Dryout?
Session 1:					
1	625	792	0.10	0.30	No
2	625	797	0.10	0.45	No
Session 2:					
3	375	698	0.40	0.60	No
4	365	700	0.40	0.90	Yes
5	360	703	0.40	1.20	Yes
6	360	705	0.40	1.20	Yes
7	465	707	0.35	0.75	No
8	460	703	0.38	1.13	No
9	545	710	0.28	0.60	No
10	540	710	0.28	0.90	No
11	550	712	0.28	1.20	No
12	640	725	0.15	0.75	No
13	640	725	0.25	1.20	No
14	355	537	0.23	0.90	No
15	360	546	0.23	1.43	No
16	445	630	0.23	1.43	No
17	550	657	0.08	1.43	No
Session 3:					
18	365	640	0.35	1.43	?
19	375	700	0.45	0.90	No
20	375	700	0.45	0.60	No
21	550	690	0.15	2.00	No
22	550	682	0.15	2.00	No
23	620	698	0.05	2.00	No
24	605	700	0.08	2.50	No
25	390	740	0.38	0.60	-
26	500	748	0.28	0.90	-
Session 4:					
27	500	552	0.05	2.50	-
28	360	560	0.38	1.50	-

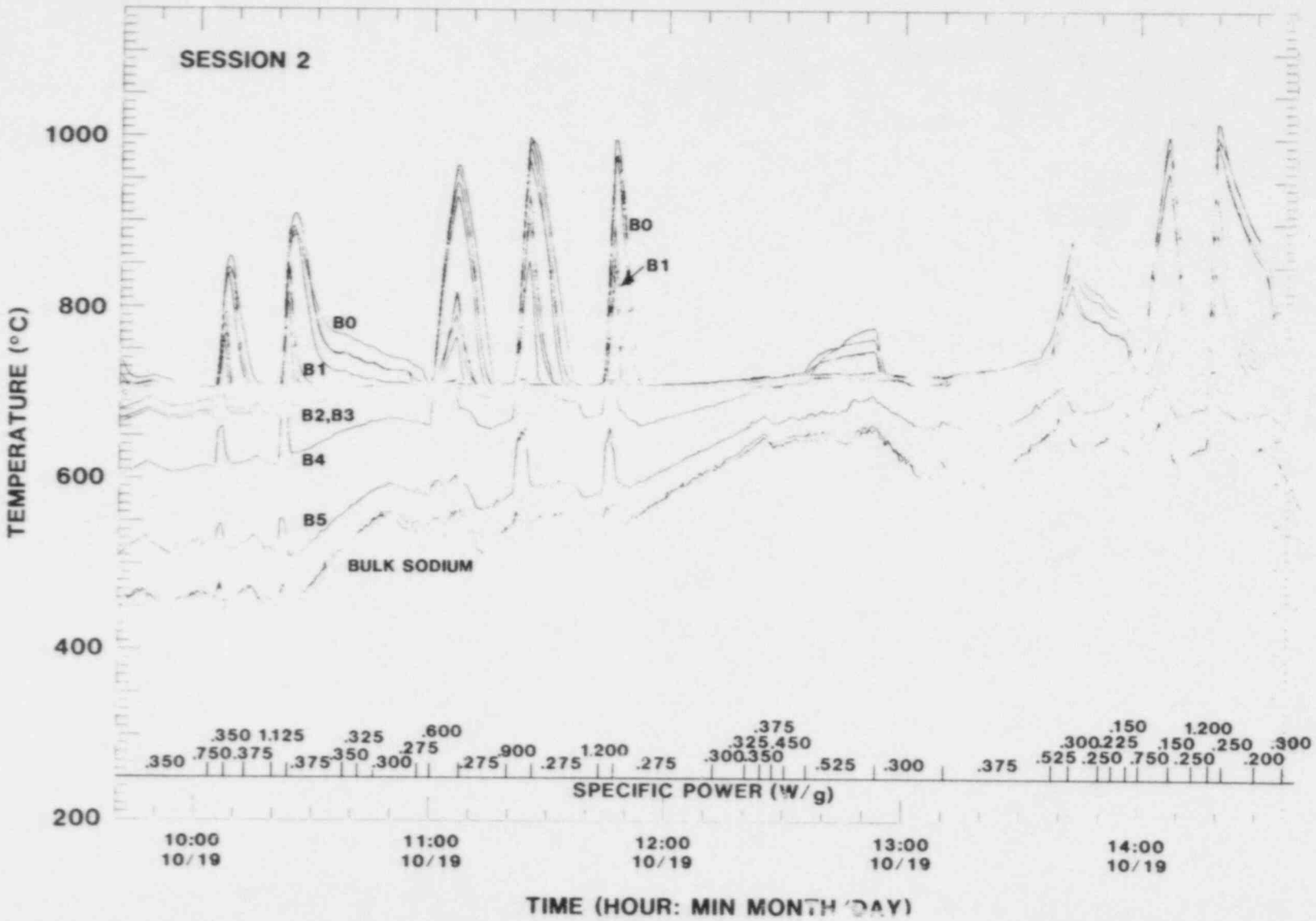

Figure 3-7. Session 2 Power Steps

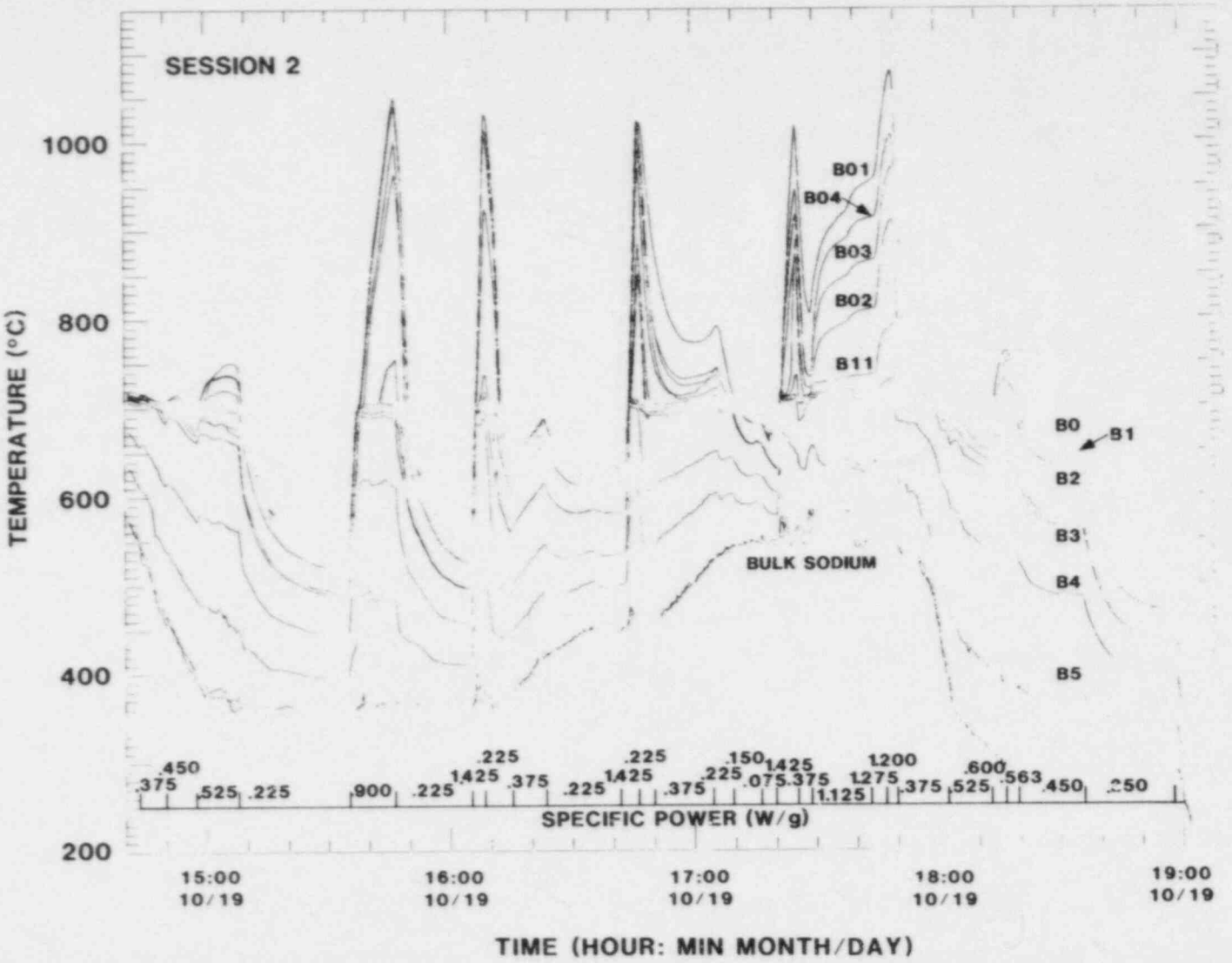

Figure 3-8. Session 2 Power Steps

zone was less than 20 mm thick, indicating that in these cases the bed was channeled. Only with large subcooling was it possible to dry out the 20-mm (B2x) level, presumably because of channel suppression. (Although steady state was never achieved at these high powers, the dry zone thickness was usually established and nearly steady well before temperature limits forced a power reduction.) Some examples will demonstrate the features of these tests.

Figure 3-9 shows the bed temperatures for power step 4. The bulk sodium temperature was 365°C and the initial subcooled zone was about 60 mm thick. A step to 0.90 W/g yielded very rapid dryout of the 1.5-mm (B0x), 10-mm (B1x), and 20-mm (B2x) levels. A slow decrease in the saturation temperature (see B3x during power step) suggests some bed loosening, but it may be a nonpenetrating channel as described in Section 3.1.5.

Figure 3-10 shows the bed temperatures for power step 10. The bulk sodium temperature was 540°C and the initial subcooled zone was only 40 mm thick. A power step to the same level as the previous example (0.90 W/g) produced dryout in the 1.5-mm (B0x) and 10-mm (B1x) levels only. Thus the bed was more coolable with reduced subcooling. This increased coolability may be due to the formation of penetrating channels.

Figure 3-11 shows the bed temperatures for power step 14. The bulk sodium temperature was nearly the same as in power step 4, but the bed power was chosen to be lower so as to start the step well below boiling. When the power was increased to the same level as in the previous two cases, a sharp drop in temperatures occurred just before dryout. In this case, the drop represented flashing of superheated liquid sodium. Comparison of the response of the temperatures in the subcooled zone to that in power step 4, indicated that the flash released a large amount of vapor. This very large vapor flow may have disrupted the bed and established a penetrating channel. Evidence for this was that the dry zone temperatures were much less than in power step 4 and the 20-mm (B2x) level did not dryout. Thus, with the additional effect of flashing, a highly subcooled bed may channel and be more coolable.

The implication of having a dry zone which is limited to 20 mm under prototypic heating is that the maximum temperature will be less than the melting point of UO_2 (based on conduction calculations). Unfortunately, it will be above the melting point of steel. Furthermore, this result applies only to stratified beds the height of the D9 bed. Thicker stratified beds that channel will have a larger limit to their dry zones. This is because the dry zone is limited by the bottom of the channels, and channel lengths are limited by the particle diameter at a given level and

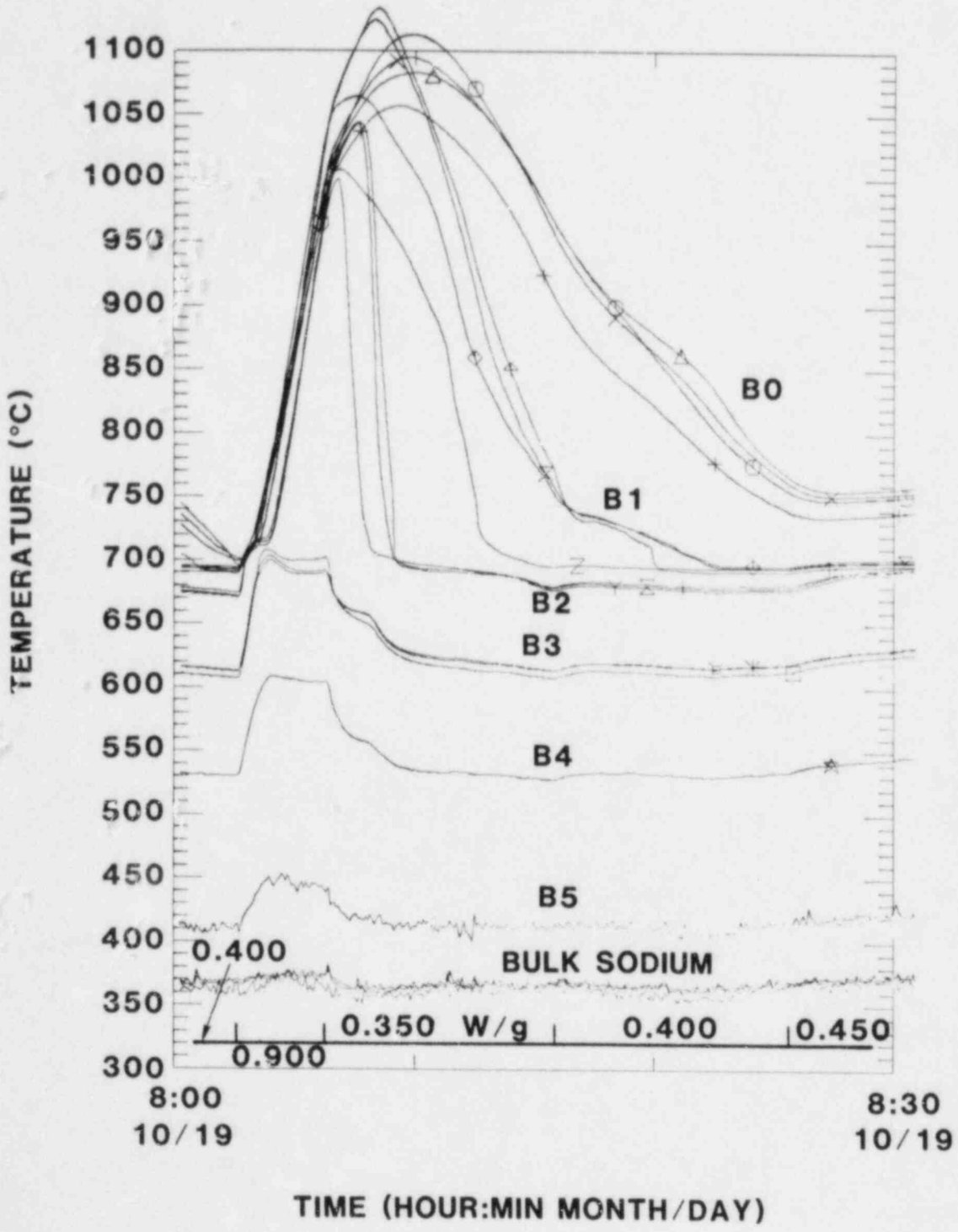

Figure 3-9. Session 2 Bed Response to Power Step (Power Step 4)

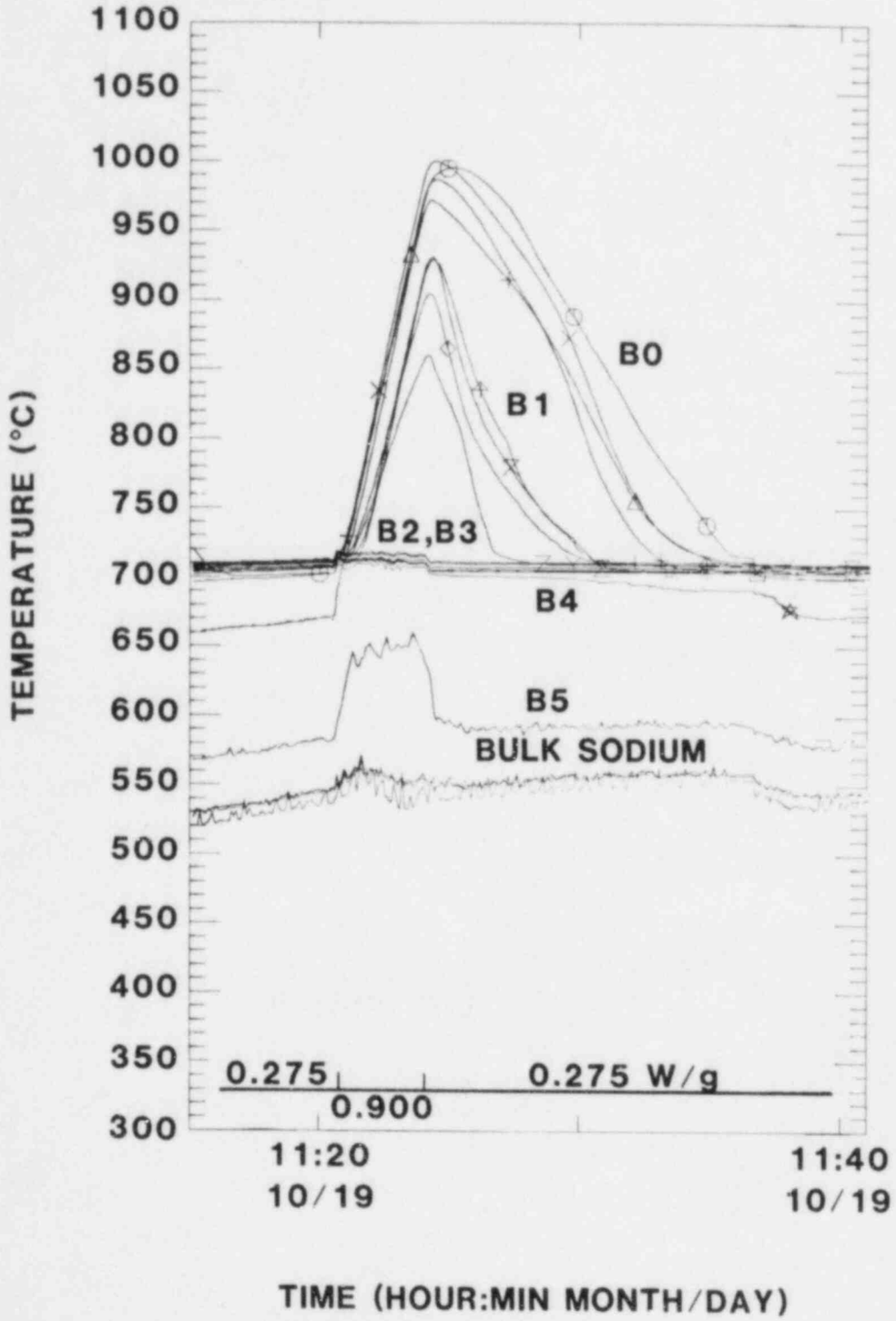

Figure 3-10. Session 2 Bed Response to Power Step (Power Step 10)

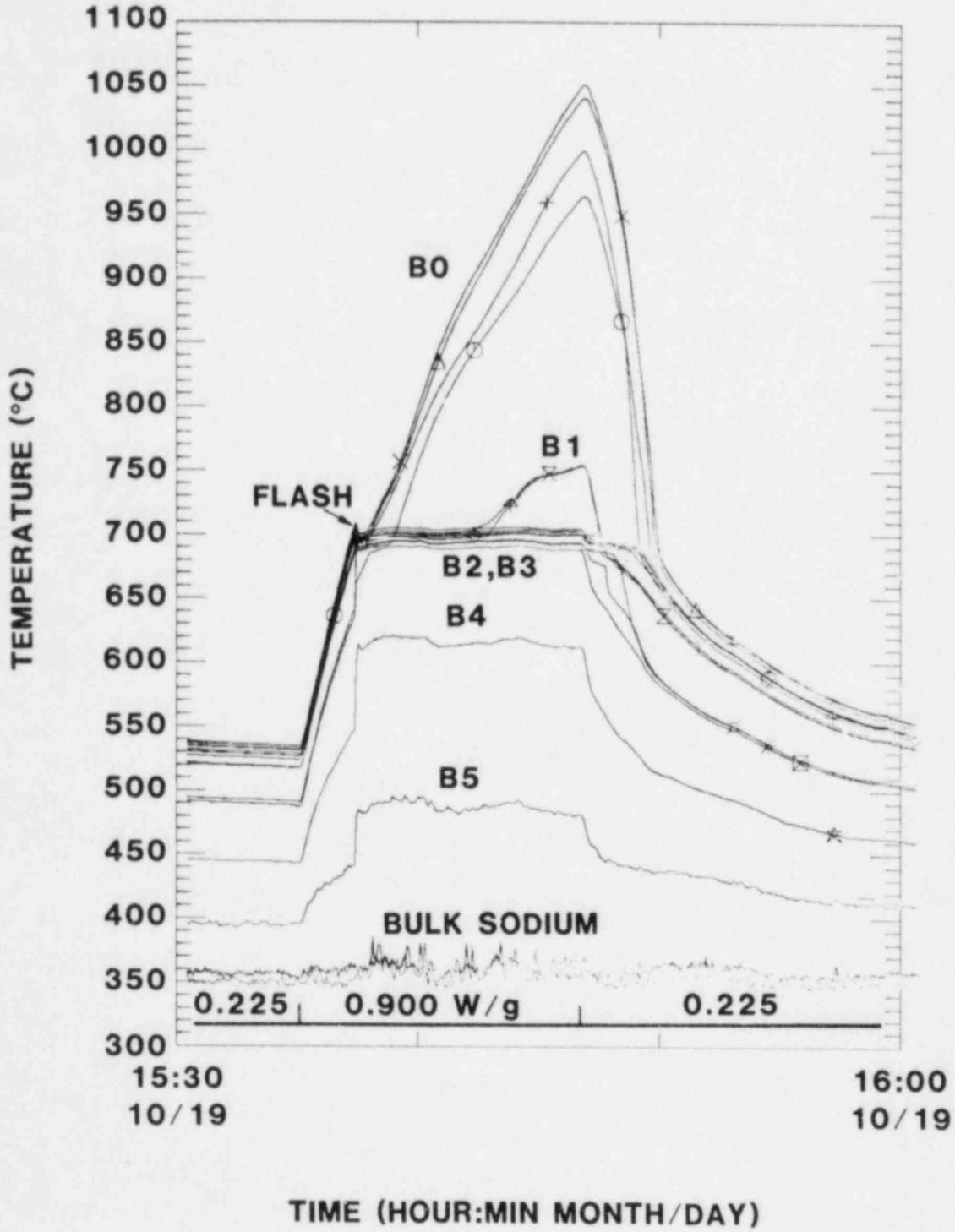

Figure 3-11. Session 2 Bed Response to Power Step (Power Step 14)

the weight of the bed above that level. Thus, although the power-step series indicated a state of increased coolability with more prototypic heating, the increase was not significant.

3.2.3 Session 2 Dryout Measurements

In the second session, 13 incipient dryout points were determined between the large power-step tests. As shown in Figure 3-12, the dryout powers indicated by data points 11-14 and 18-23 were slightly higher (about 30 percent) than during the first session. These differences may be attributed to minor changes in the bed structure, manifested primarily by an increase in the power required for incipient boiling. Dryout still occurred within 20 percent of incipient boiling, indicating that in spite of the many large power step tests, the bed remained sufficiently stratified to greatly suppress the dryout power.

Even though most of the dryout points indicated low dryout powers, some showed abnormally high powers. These dryout points were transitory in nature and are labeled "T" in Table 3-1 and in Figure 3-13. These measurements were made shortly after a large power step test and it is believed that the bed had not settled completely. The sequence of points 15 to 18 shows how the dryout flux decreased over a period of 90 min. The one-dimensional model predicts that the dryout power in a stratified bed will be greater if the porosity increases with elevation so as to compensate for the decreasing particle size. The power step may have expanded the bed in such a way to cause an increased dryout flux, and then the bed settled with time and boiling.

3.2.4 Session 2 Channel Formation

During the many power steps in the second session, channel formation occurred in all cases except those with the highest subcooling. Apparently, the channels can be suppressed if the subcooling is sufficiently large and the power is low. When the channels formed, the 20-mm (B2x) level remained in the boiling zone as predicted by the pretest calculations.[3]

3.2.5 Session 2 Flashing

Since some of the power steps were made from subcooled initial conditions, it was anticipated that a superheat flashing event would occur. The pretest predictions had indicated that the amount of superheat should be nearly equal to the degree of subcooling if the subcooling was not too large.[9] However, in all cases the amount of superheat was 30°C or less (e.g. Figure 3-11) even though the subcooling was as large as 180°C and the bed had been continuously

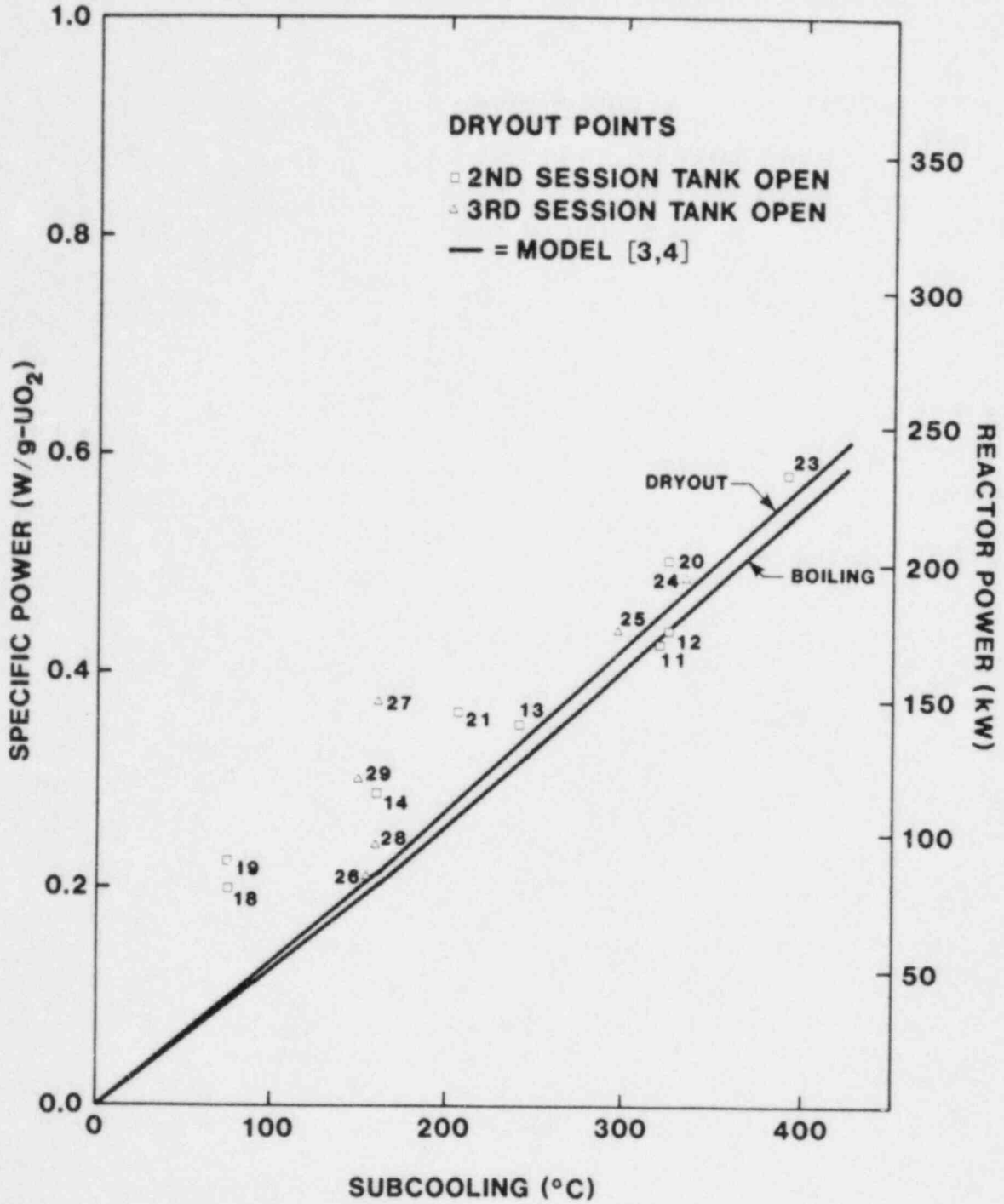

Figure 3-12. Sessions 2 and 3 Incipient Dryout Measurements

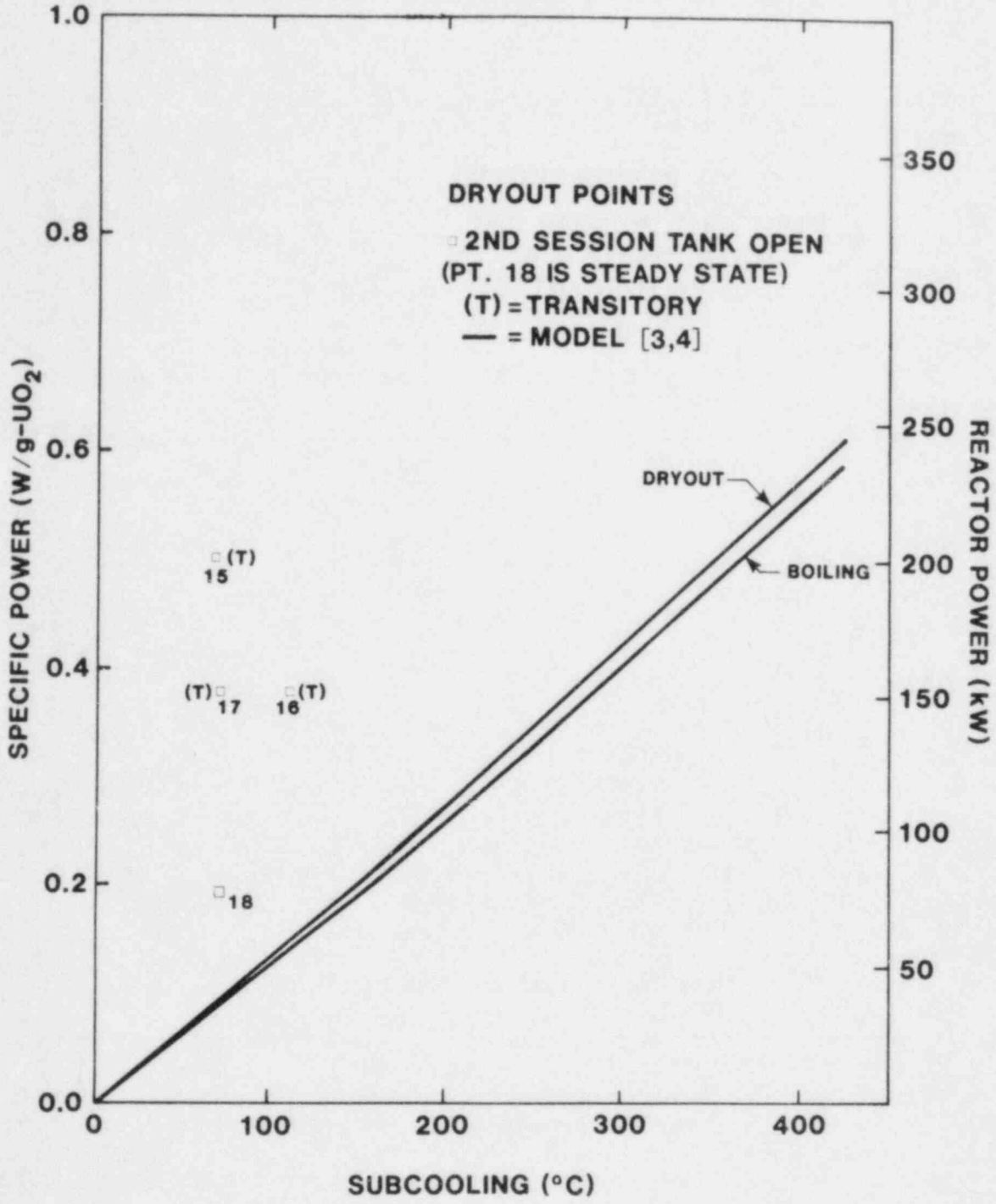

Figure 3-13. Transitory Dryout Measurements

boiled for over 8 hr prior to the first flash. Possibly, the rapid heating caused boiling to be initiated near the middle of the bed where active nucleation sites were still present.

Another unexpected result was obtained at the first onset of boiling in the second session (Figure 3-6 at ~06:48). Since the bed had been subcooled after boiling during the first session, a superheat flashing event was again anticipated. However, upon heating the bed to the boiling temperature, boiling was initiated and no flash was observed. The lack of a flash may be due to cover gas leaking into the bed along shrinkage cracks that formed when the bed was frozen between sessions. The gas then provided nucleation sites that reduced the superheat to undetectable levels. Flashing did not occur at the beginning of any of the sessions. This result is important for future tests which need to run over many days.

3.2.6 Bed State at the End of Session 2

The control run at the end of Session 2 (Figure 3-8 at 18:50-18:58) indicated that the bed thickness was essentially unchanged during Session 2. The top thermocouple (B5) indicates a small change in the bed surface, but the lower thermocouples do not indicate any integral change in bed height.

3.3 Session 3

The third session was concerned with performing extended dryout studies. In these studies incipient dryout was first attained and then the power was slowly increased, so that the growth of the dry zone could be monitored. Also, the pretest predictions had shown that at certain power levels, channels would form that would subsequently reduce the size of the dry zone. Hence, by performing very careful extended dryout studies these phenomena could be observed.

In addition to the dryout studies, an attempt to produce a superheat flashing event was also made. As described below, this attempt was successful and a 90°C flash was obtained. After the flash, the incipient dryout power was determined to be approximately 4.4 W/g, which was 20 times larger than previous dryout powers at the same subcooling. This indicated that the bed geometry and stratification were significantly altered.

3.3.1 Session 3 Dryout and Channeling Investigations

During the third session, an extended dryout investigation was performed (Figures 3-14, 3-15, 3-16, and 3-17). This study explored the growth of the dry zone as power increased and the shrinkage of the dry zone upon channel formation.

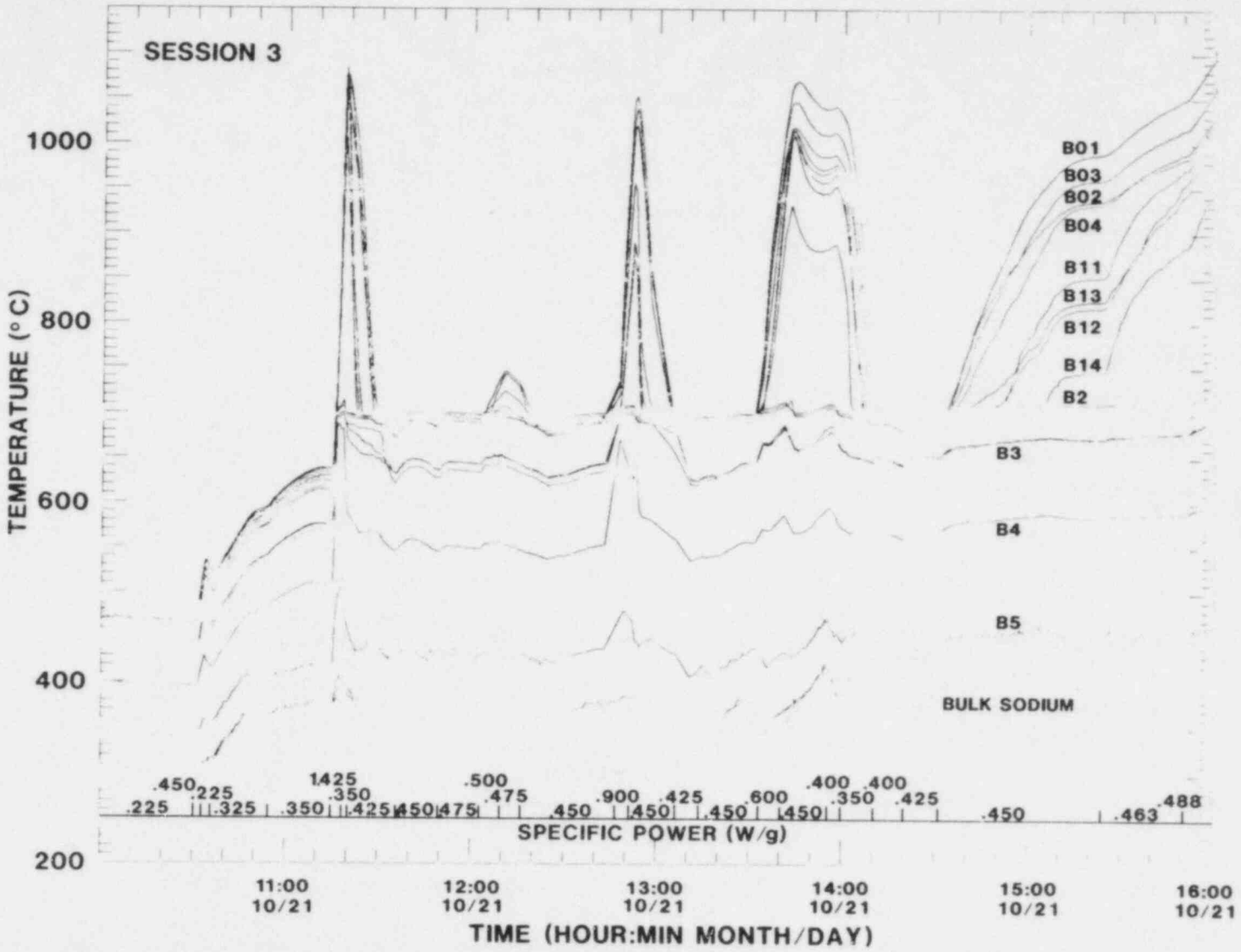

Figure 3-14. Session 3 Power Steps

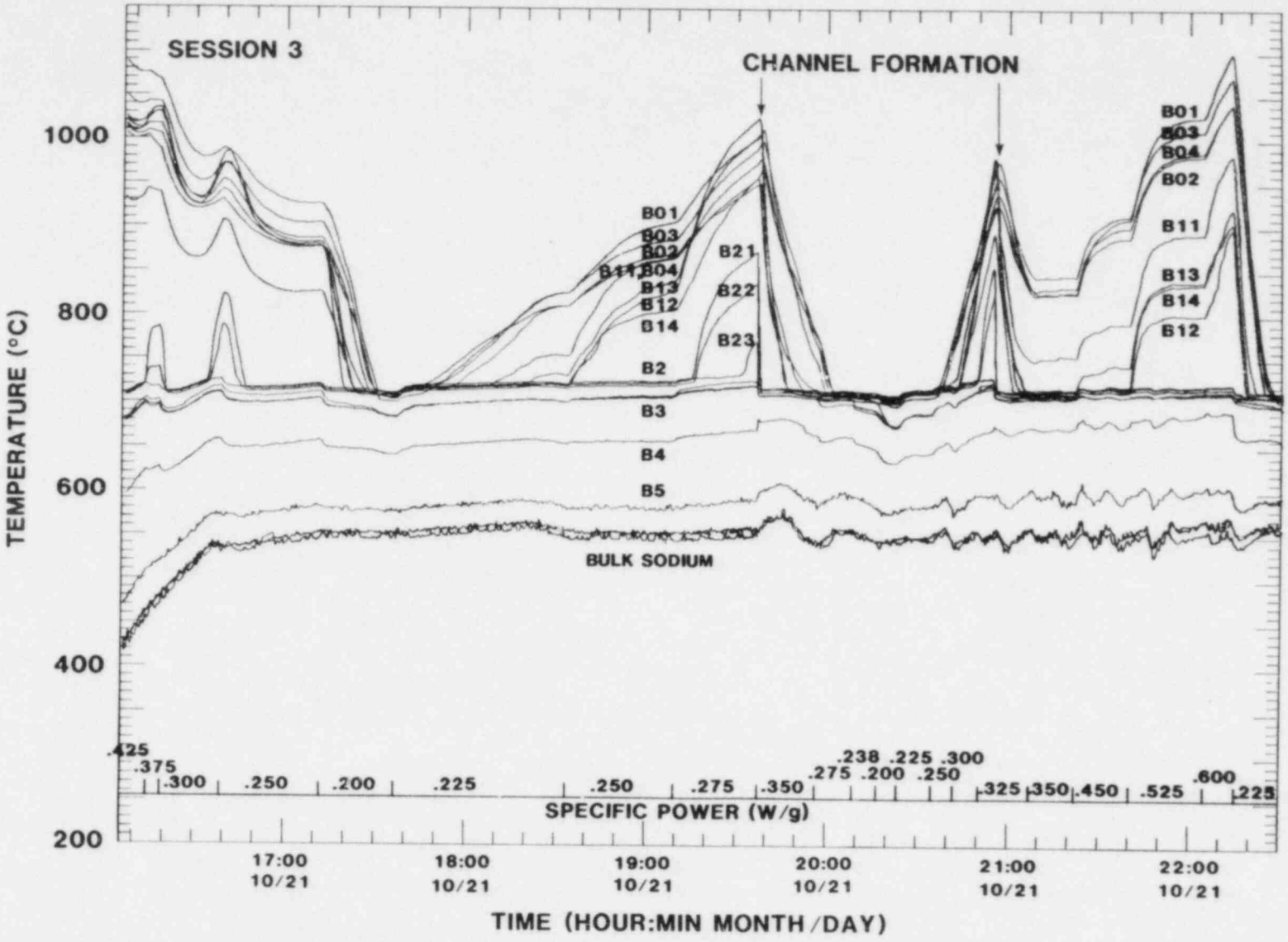

Figure 3-15. Session 3 Dryout and Channel Formation

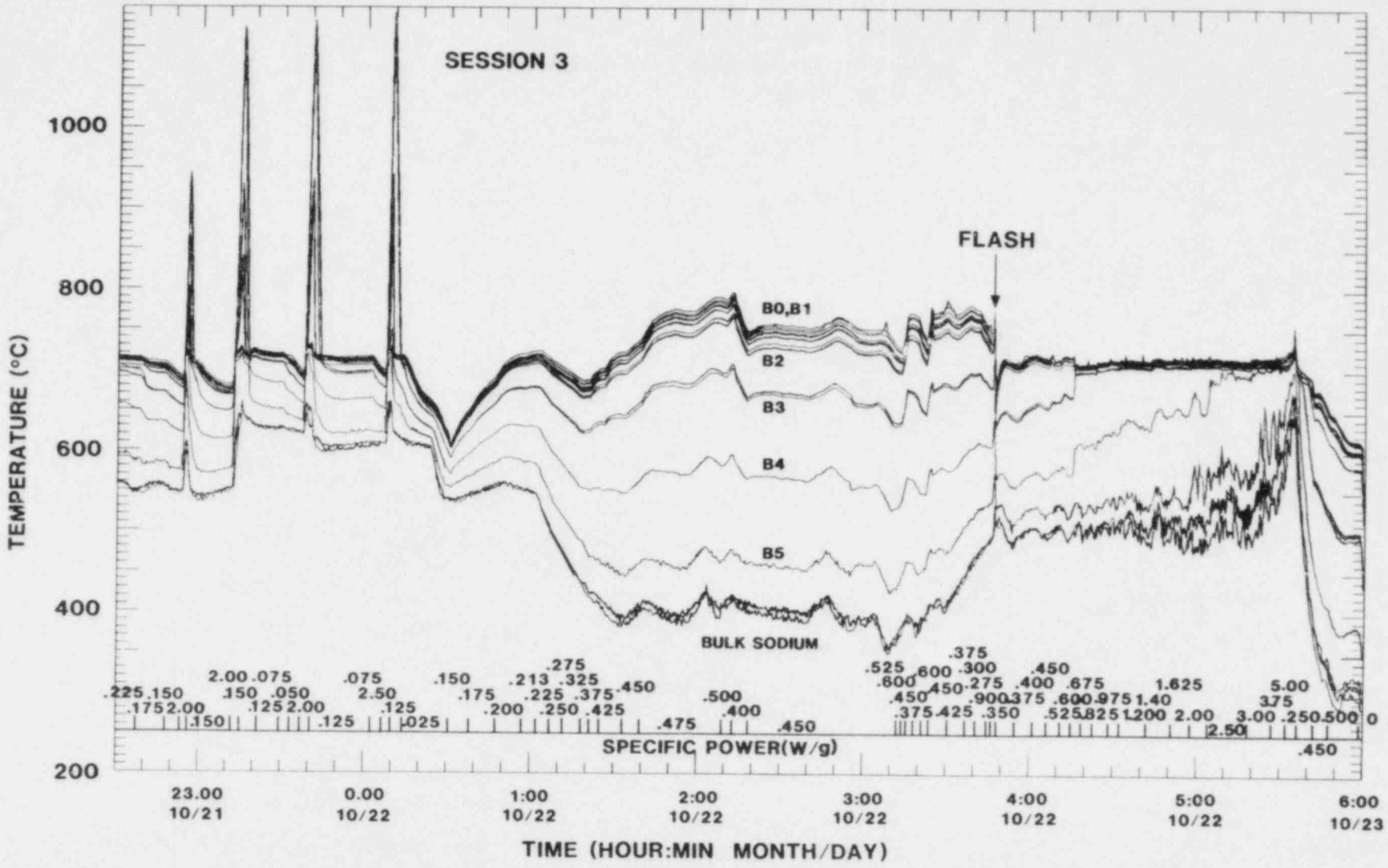

Figure 3-16. Session 3 Flash and Subsequent Dryout

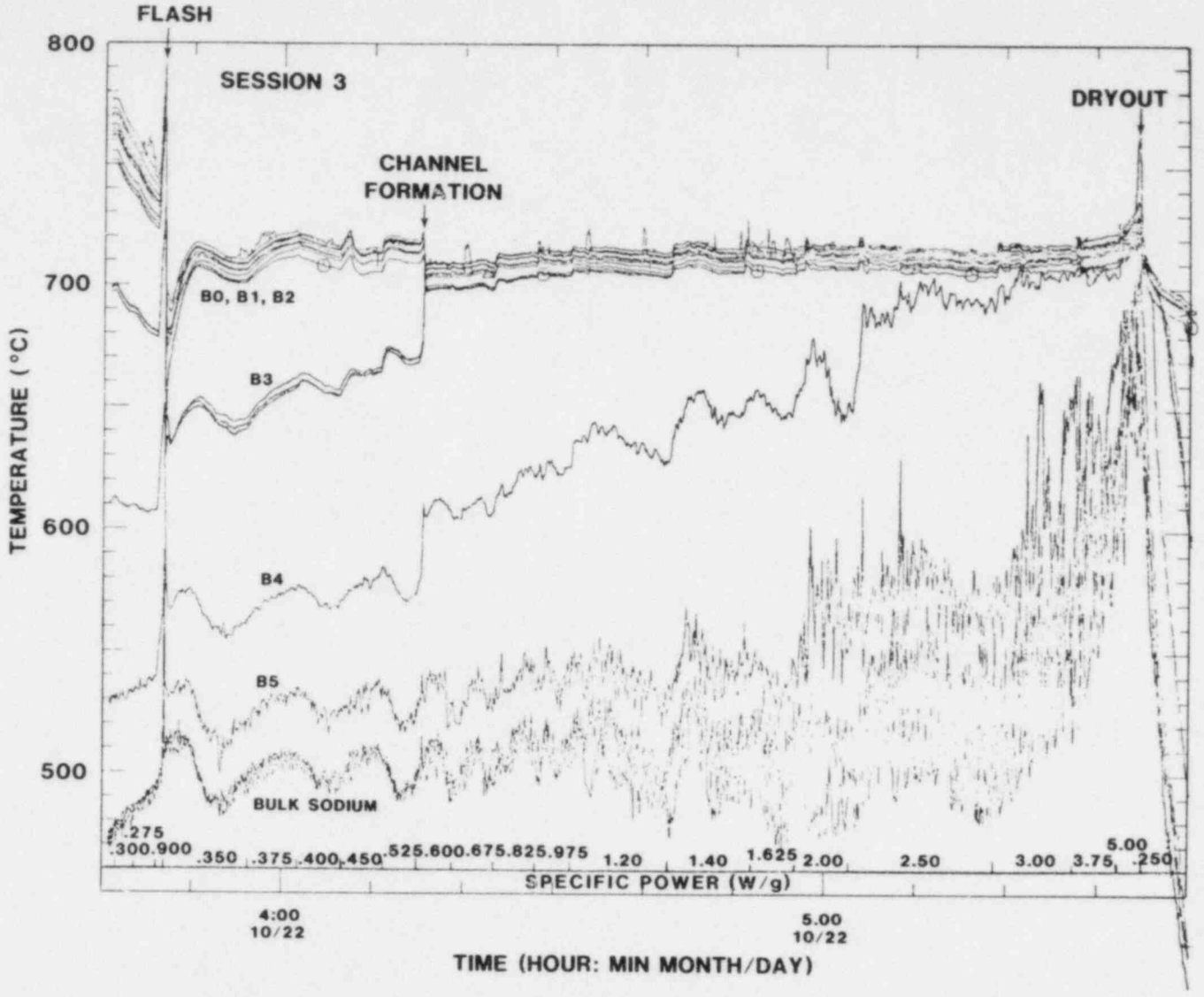

Figure 3-17. Session 3 Flash and Subsequent Dryout

Incipient dryout measurements made in this study were slightly higher than in previous sessions. Again, these differences were probably due to changes in the bed structure (i.e., porosity and height changes).

The pretest predictions had indicated that channeling would only occur after dryout and when it occurred the dry zone thickness would decrease. Figure 3-18 illustrates the anticipated thicknesses of the subcooled, boiling, and dry zones as a function of power (based on a 77-mm thick bed).

During the extended dryout study, channeling occurred after dryout and reduced the dry zone thickness as predicted. This phenomena can be more clearly seen in Figure 3-15 (18:00 to 20:00). The thermocouple readings before the channel formation show that the dry zone extended above the 20-mm (B2x) level. After the channel formation, the temperatures dropped rapidly and the 20-mm (B2x) level was then in the boiling zone. This drop in temperature is a clear indication that the dry zone thickness decreased. Indeed, it appears that the dry zone would have eventually disappeared entirely with sufficient time. This is greater coolability than predicted, but as seen in Figure 3-18, the channeling after dryout behavior was qualitatively predicted correctly.

Further study showed that the channel formation phenomenon was reversible and repeatable. Figure 3-15 (20:00 to 23:00) shows that initially the channel was suppressed, and the bed dried out at approximately the same power. Furthermore, at essentially the same power level, a channel formed and the bed temperatures dropped. The temperatures after channel formation were slightly higher in this case, indicating some hysteresis, but this is probably a minor point. The observation of repeatable channel formation and collapse suggests that the bed was wetted and that the hypothesis of channel suppression by subcooling (as evolved from and supported by previous D-series experiments) is correct.

3.3.2 Session 3 Flashing

In the previous sessions, the superheat flashing events were either nonexistent or significantly reduced relative to their predicted values. At the start of the third session, again no flash occurred when boiling was first attained. Hence, after the extended dryout study was completed, a careful attempt was made to produce a superheat flashing event.

To perform this study, the bed was first substantially subcooled (100°C) and then slowly raised to the boiling temperature. The power was increased slowly and temperatures rose above the boiling temperature. A maximum

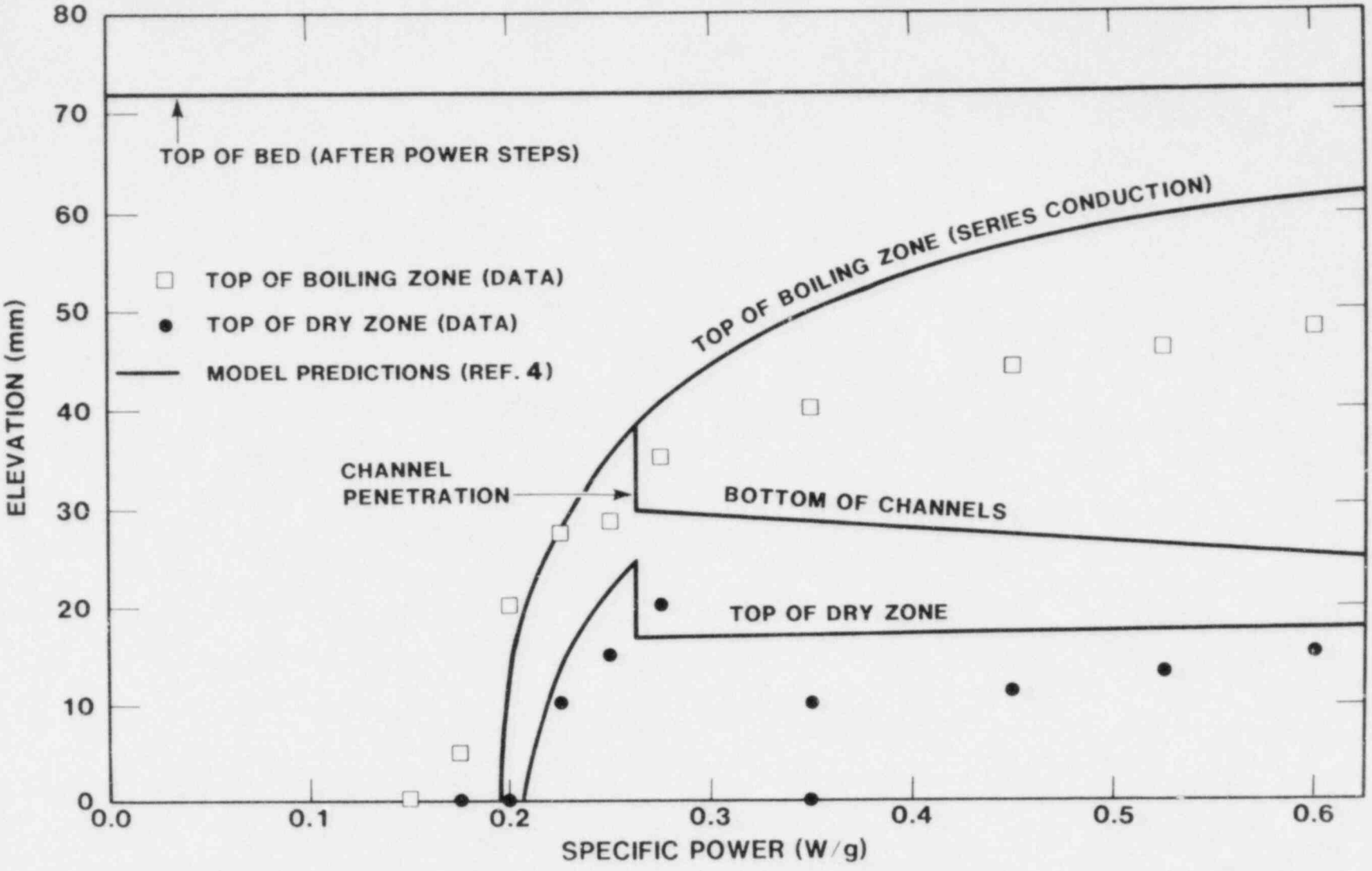

Figure 3-18. Session 3 Zone Thickness Predictions and Measurements

superheat of 100°C was obtained before reducing power for safety reasons. Attempts were then made to initiate the flashing event. After several attempts a 90°C flash was initiated (Figures 3-16 and 3-17). A flash of this magnitude was higher than anticipated and may be a result of the long boiling times prior to the flash.

After achieving the flash, the incipient dryout power was investigated. The bed appeared to be packed at first, as evidenced by the large span of saturation temperatures in the bed (Figure 3-17 at ~03:50-04:10). Similar behavior was seen in D5.[8] As the power was increased, a channel formed (at 04:16) before dryout was reached. Subsequent power increases yielded more channels, and the dryout power was eventually determined to be approximately 4.4 W/g. This was the last dryout measurement to be made in this experiment. Apparently, the large flashing event mixed the bed considerably, thereby negating the effects of stratification. With a mixed bed, channels could penetrate to the bottom of the bed resulting in the dramatic increase in the dryout power.

3.3.3 Bed State at the End of Session 3

The control run at the end of Session 3 (Figure 3-16 at 05:55-05:58) showed that the bed height decreased about 12 mm to 65 mm or less (Figure 3-1). Evaluation of temperature profiles during Session 3 indicate that about half of this change occurred during the first large (90°C) flashing event and half during the strong boiling (with low subcooling) during the subsequent search for incipient dryout after the flash (Figure 3-17). This large change indicated that a fraction of the original bed was outside of the crucible at the end of this session. The thermocouples below the crucible exhibited a larger response to a step increase in power at the start of Session 4. Their response was consistently much smaller prior to the 90°C flash. This supported the idea that there was fuel outside the crucible, and indicated that most of it left the crucible during the flash and the subsequent high-power boiling.

3.4 Session 4

The fourth session investigated the flashing phenomenon. As found in the third session, a large flash could disrupt the bed to such an extent that the dryout power increased by a factor of 20. Hence, it was important to gain a better understanding of this phenomenon in a systematic manner.

A large number of flashing events were initiated in this study. However, the maximum superheat attained was only 70°C. The 90°C flash could not be repeated. On the whole, the magnitude of the flashing events followed the theoretical curve if sufficiently long boiling times were used. If

short boiling times were used the superheat was substantially reduced.

3.4.1 Session 4 Dryout Measurements

A search for dryout was made at the start of Session 4 with 300°C bulk sodium (Figure 3-19). Several channel events were observed as the power was increased. No dryout was observed up to 1.28 W/g. Higher powers were not attempted because vigorous channeled boiling could have disrupted the bed more. The fact that the bed was coolable at a power of 1.28 W/g demonstrated that the bed disruption caused by the 90°C flash at the end of Session 3 was a permanent change.

3.4.2 Session 4 Flashing

Most of Session 4 was devoted to investigating the superheat flashing phenomena (Figures 3-20 and 3-21). Figure 3-22 illustrates the measured superheats at which flashing occurred. The theoretical values are also plotted.[3,9] Three classes of measurements are presented: those in which the saturation temperature was exceeded during a large power step test, and those involving only small power increments with either more or less than 15 min of boiling since the last flash. The measurements that agree well with the prediction were obtained with small steps after allowing the bed to boil for a period of time (15 min) prior to that flash. (Note that all these data occurred after the many hours of initial boiling in Session 1.) The values that lie beneath the curve were either boiled for shorter times or subjected to large power steps. Apparently, both the boiling history and the heating mode are important for the creation of a large flashing event.

3.4.3 Bed State at the End of Session 4

The control run made at the end of the fourth session gave essentially the same results as the run at the start of the session. This indicated that the bed height was unchanged during Session 4.

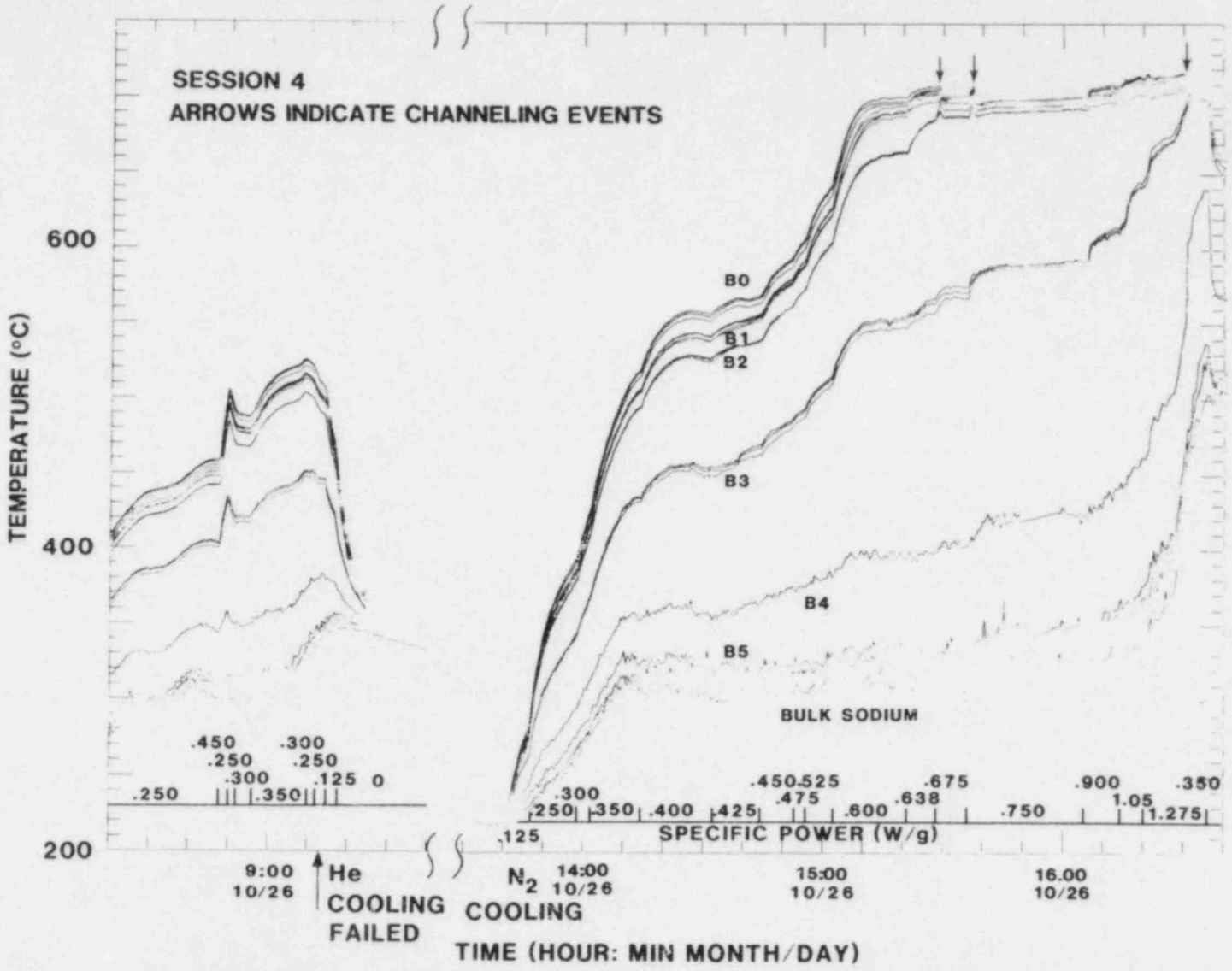

Figure 3-19. Session 4 Search for Dryout

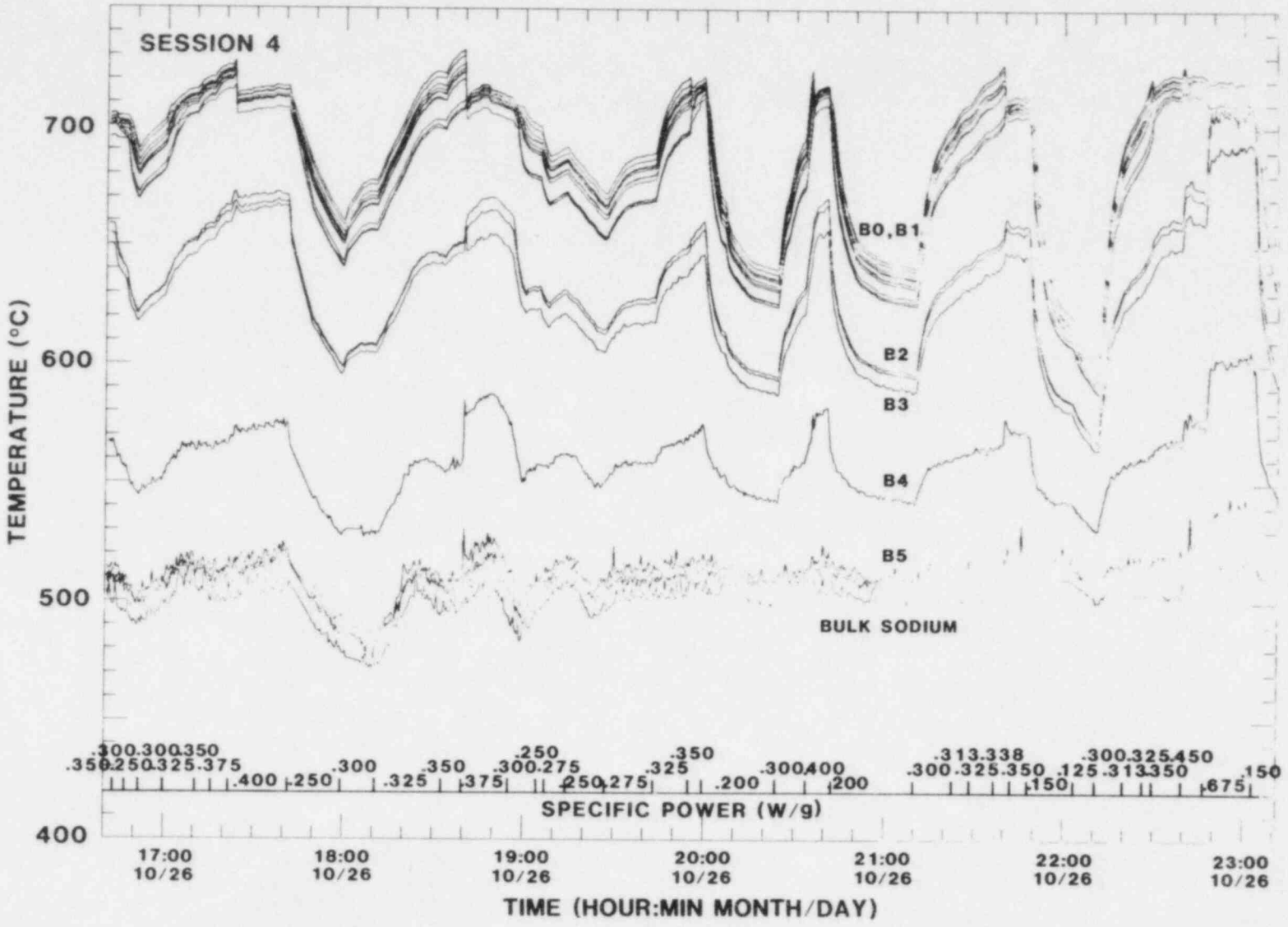

Figure 3-20. Session 4 Flashing

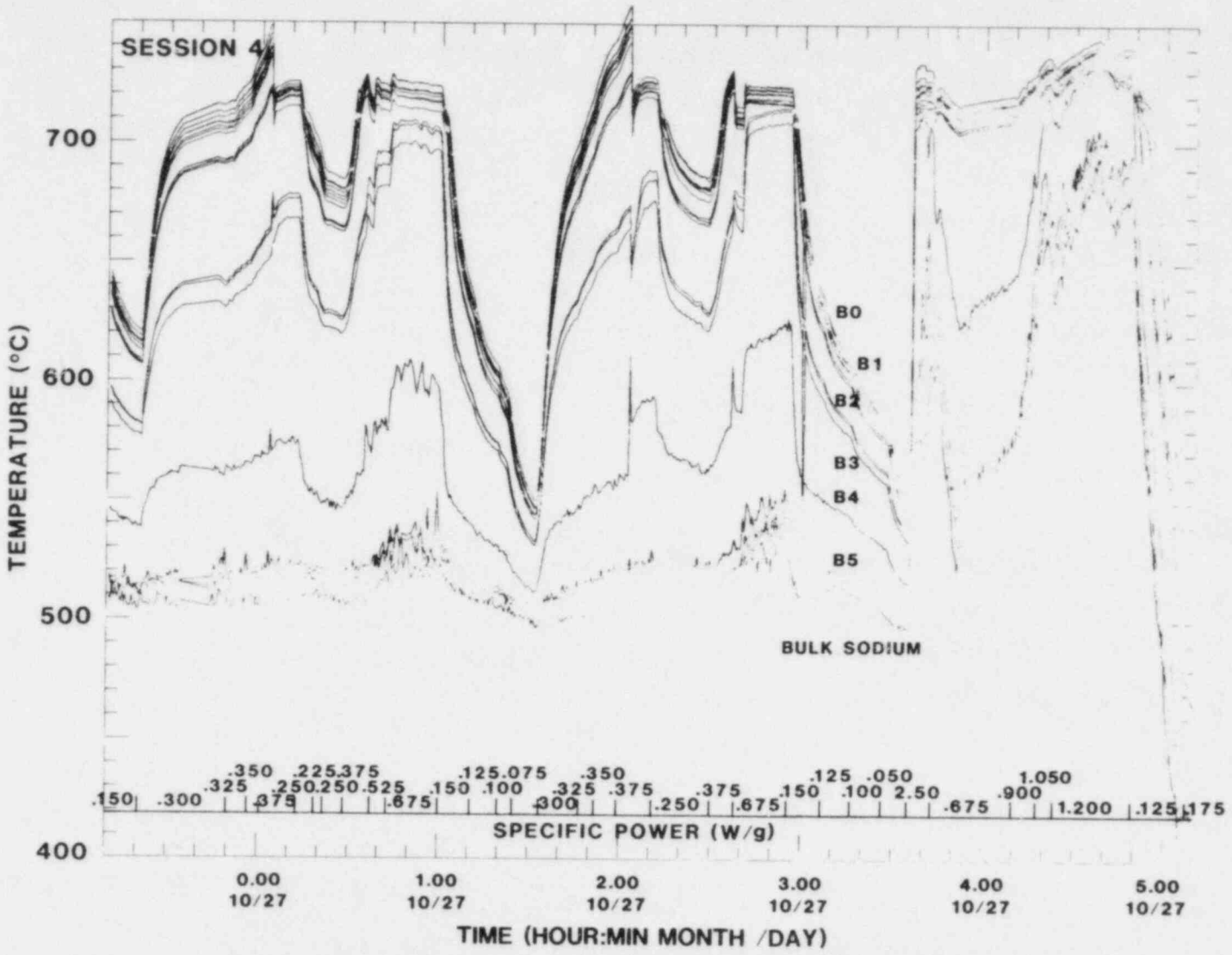

Figure 3-21. Session 4 Flashing

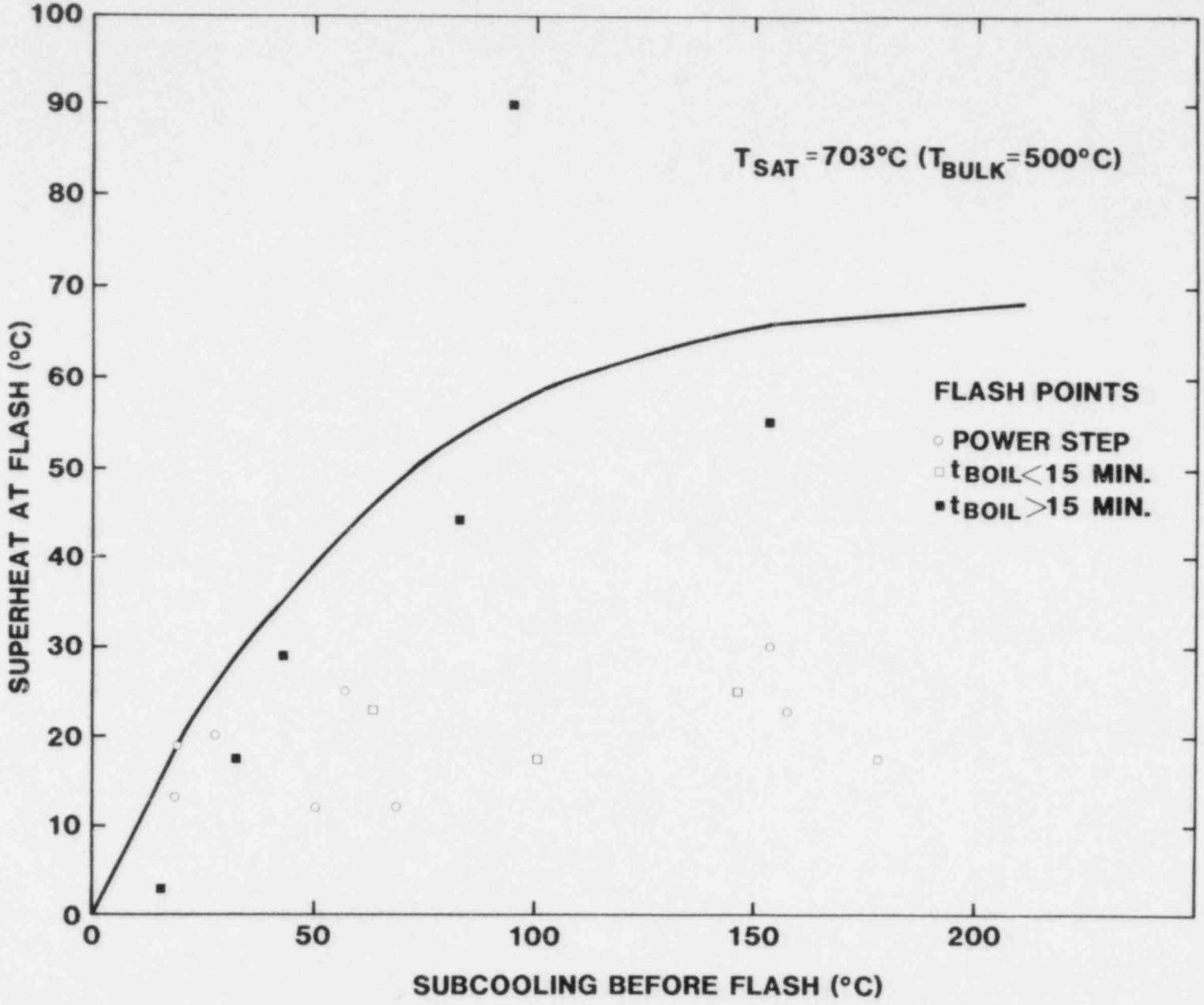

Figure 3-22. Superheat at Flashing

4. POSTTEST X-RAYS

X-rays were taken of the experiment following the completion of the test (Figures 4-1 and 4-2). The bed height varied from approximately 53 to 61 mm with an average height of 57 mm, confirming the observation of an apparent decrease in bed height at the end of Session 3. The original bed height was 77 mm; therefore, the average bed height decreased by approximately 20 mm. Based on the observed temperature profiles during control runs, this occurred primarily during the 90°C superheat flashing event and the strong boiling during the subsequent search for incipient dryout. Some of the UO_2 which left the bed settled on the top flange of the crucible. Most of the UO_2 particulate, as evidenced by the x-rays, was located in the region below the crucible.

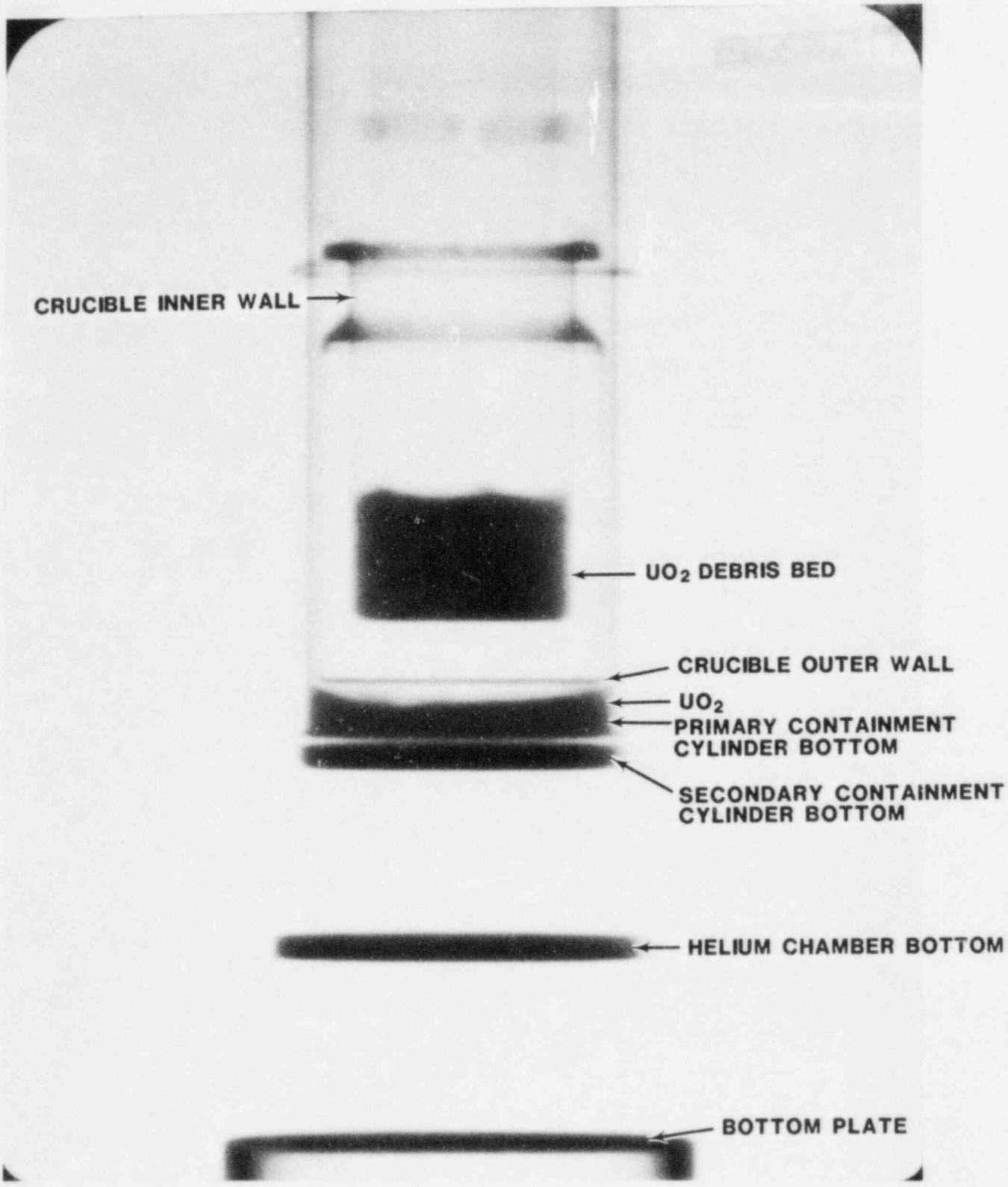

Figure 4-1. Posttest X-ray of D9

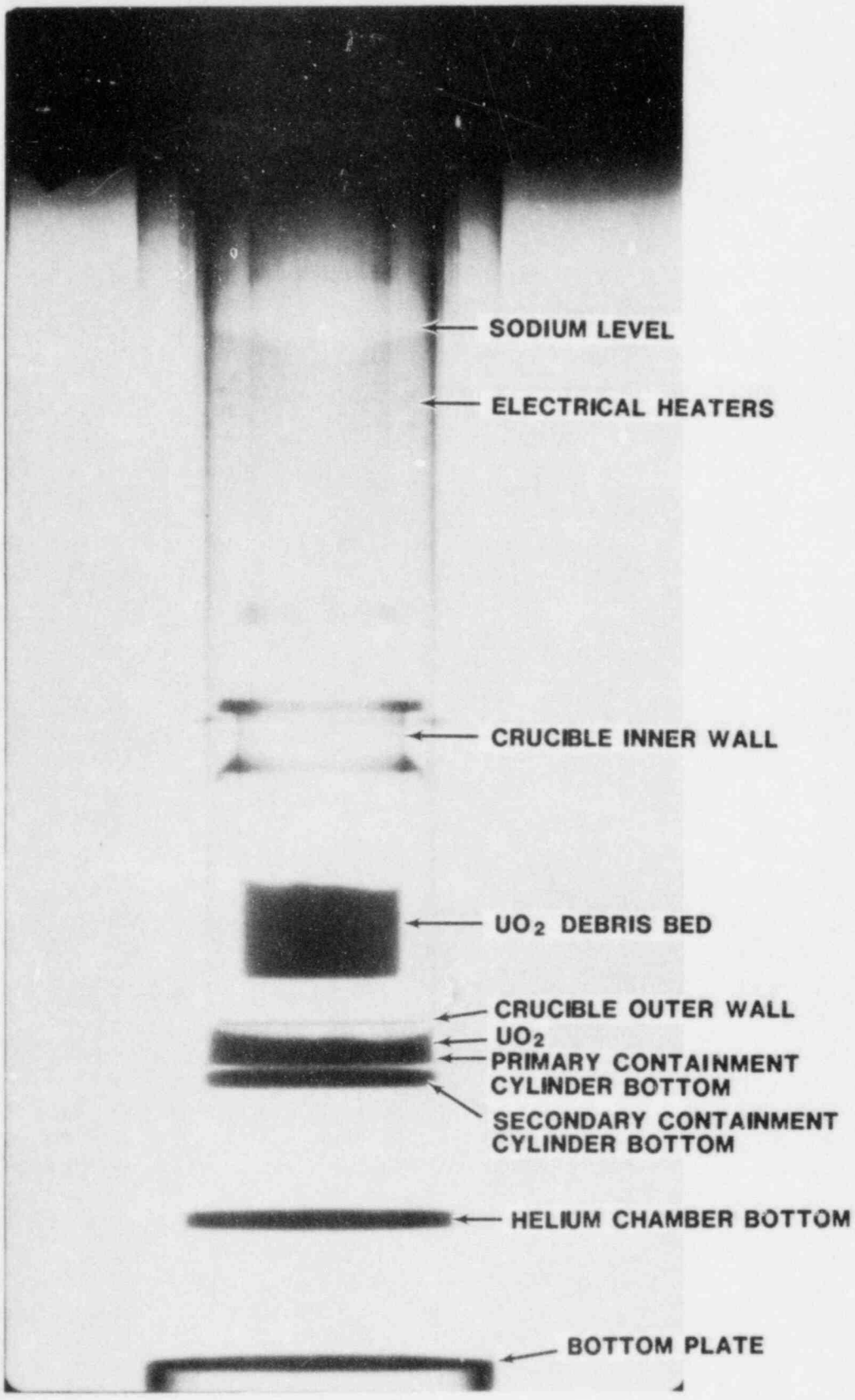

Figure 4-2. Posttest X-ray of D9

5. SUMMARY

The D9 experiment provided significant new data on the coolability of debris beds. This data will be extremely valuable for validating models needed in assessing reactor safety.

The data largely consisted of dryout measurements for a shallow, stratified urania bed; however, other debris-bed phenomenological data related to channeling, extended dryout, and superheat flashing were also obtained. From these data a number of conclusions can be drawn.

The most significant result of the experiment was that incipient dryout occurred in the debris bed at extremely low specific power levels, ranging from 0.10 to 0.58 W/g. In fact, dryout always occurred at power levels just above the boiling power level. This result, which was predicted by Lipinski,[4] implies that if a stratified bed, even a very shallow one, begins to boil, then it is likely that dryout will occur.

In previous experiments, (e.g., Reference 5) the formation of vapor channels in a debris bed was found to increase the coolability of the bed. However, in D9 there was no clear evidence that channeling ever occurred before dryout was attained. Even at the lowest subcooling level attained during the incipient dryout investigations, no vapor channels formed. Rather, only a loosening of the bed, due to capillary pressure relief, was detected. Also, during the large power step investigations, dryout always occurred before any vapor channels were detected. In fact, for all cases prior to the bed-disrupting superheat flashing event, channeling only occurred after dryout and the channels did not penetrate to the bottom of the debris bed.

Consequently, the full benefit of channels (order of magnitude change in coolability) did not occur. This effect of "channeling after dryout" and the failure of the channels to completely penetrate the bed, were both in excellent agreement with the Lipinski model.[4] Therefore, in a shallow, stratified debris bed, even with channeling, dryout (and, hence overheating) will occur. Incipient dryout powers ranged from 0.10 to 0.64 W/g which is well below the dryout power expected during in-vessel portions of the accident scenarios.

During the extended dryout investigations, the dry zone thicknesses were fairly close to those predicted by the one-dimensional model.[3,4] In addition, a small increase in power yielded a collapse of the dry zone with low subcooling. This was the most direct indication of channeling in the experiment. It was repeatable and occurred at only

slightly higher powers than predicted. The modeling could predict the extended dryout behavior and, hence, this data provided validation of the model.

The investigations into flashing, while perhaps not directly applicable to reactor safety, did reveal that this phenomenon could significantly alter the debris bed characteristics. As evidenced by the 90°C superheat flashing event, the stratification in the bed was completely changed following this event. This left the bed in a state which allowed complete channel penetration and a factor of 20 increase in the dryout power. This large dryout power is typical of a shallow uniform bed which would be coolable in an accident situation. The subsequent studies showed that the flashing could be predicted based on theory.[9] However, questions still remain as to whether or not the proper conditions for a flashing event would occur during an accident.

Finally, it is important to note that all of the data is valuable for assessing and validating models. To a large extent, all the dryout and channeling data were well predicted by the Lipinski model.[4] The good agreement here and the fact that this model is physically based mean that this model can be used to assess coolability questions related to debris bed behavior under a variety of accident conditions.

6. REFERENCES

1. T. Y. Chu, "Fragmentation of Molten Core Material by Sodium," Proceedings of the LMFBR Safety Topical Meeting, Lyon, France (July 19-23, 1982).

2. W. E. Nelson, "Neutronic Calculations for D7 and D8," memo to Distribution, Sandia National Laboratories, Albuquerque, NM, May 20, 1981.

3. J. E. Kelly and R. J. Lipinski, "D9 Pre-Experiment Calculations," memo to C. A. Ottinger and G. W. Mitchell, Sandia National Laboratories, Albuquerque, NM, October 13, 1982.

4. R. J. Lipinski, A Model for Boiling and Dryout in Particle Beds, NUREG/CR-2646, SAND80-0765, Sandia National Laboratories, Albuquerque, NM, 1982.

5. J. E. Gronager, M. Schwarz, and R. J. Lipinski, PAHR Debris Experiment D-4, NUREG/CR-1809, SAND80-2146, Sandia National Laboratories, Albuquerque, NM, 1981.

6. G. W. Mitchell, R. J. Lipinski, and M. L. Schwarz, Heat Removal From a Stratified UO_2-Sodium Particle Bed, NUREG/CR-2412, SAND80-1622, Sandia National Laboratories, Albuquerque, NM, 1982.

7. G. W. Mitchell, C. A. Ottinger, and R. J. Lipinski, The D7 Debris Bed Experiment, NUREG/CR-3198, SAND82-0062, Sandia National Laboratories, Albuquerque, NM, 1983.

8. R. J. Lipinski, "D5 Interpretation and Speculation," memo to R. L. Coats, Sandia National Laboratories, Albuquerque, NM, March 10, 1982.

9. M. Schwarz, memo to W. J. Camp, Sandia National Laboratories, Albuquerque, NM, December 15, 1980; R. E. Holtz, The Effect of the Pressure-Temperature History Upon Incipient Boiling Superheats, ANL-7184, Argonne National Laboratory, Argonne, IL, 1966.

10. J. B. Rivard, Postaccident Heat Removal: Debris-Bed Experiments D-2 and D-3, NUREG/CR-0421, SAND78-1238, Sandia National Laboratories, Albuquerque, NM, 1978; J. B. Rivard and R. L. Coats, "Post-Accident Heat Removal: An Overview of Some In-Vessel Safety Considerations," Proceedings of the International Meeting on Fast Reactor Safety Technology, Seattle, Washington (August 19-23, 1979).

DISTRIBUTION:

U.S. Government Printing Office
Receiving Branch (Attn: NRC Stock)
8610 Cherry Lane
Laurel, MD 20707
(250 copies for R7)

Division of Accident Evaluation (8)
Office of Nuclear Regulatory Research
U.S. Nuclear Regulatory Commission
Washington, DC 20555
Attn: C. N. Kelber
M. Silberberg
R. W. Wright (5)
G. Marino

Joint Research Center (12)
Ispra Establishment
21020 Ispra (Varese)
Italy
Attn: R. Klersy
H. Holtbecker
H. Meister
D. Schwalm
K. Mehr
P. Fasoli-Stella
P. Schiller
O. Simoni (5)

Power Reactor & Nuclear Fuel (10)
Development Corporation (PNC)
Fast Breeder Reactor Development
Project (FBR)
Minato-Ku, Tokyo
Japan
Attn: T. Aoki
T. Kitahara
Y. Mimoto
K. Mochizuki
H. Nakamura
M. Saito
K. Takahashi
N. Tanaka
A. Watanabe (2)

Monsieur A. Schmitt
IPSN/DSN
CEN Fontenay-aux-Roses
Boite Postale N° 6
92260 Fontenay-aux-Roses
France

DISTRIBUTION (continued)

Safety Studies Laboratory/DSN (6)
Commissariat a L'Energie Atomique
Centre d'Etudes Nucleaires de Cadarache
B. P. 1, 13115 Saint-Paul-lez-Durance
Bouches-du-Rhone
France
Attn: M. Schwarz
M. Bailly
M. Meyer Heine
M. Penet
G. Kayser
C. LeRigoleur

Centre d'Etudes Nucleaires de Grenoble (2)
B. P. 85 Centre de Tri
3401 Grenoble Cedex
France
Attn: M. Costa/STT
D. Rousseau/Pi-SEDTI

UKAEA (4)
Safety and Reliability Directorate
Wigshaw Lane
Culcheth
Warrington, WA3 4 NE
England
Attn: M. Hayns
R. S. Peckover
B. D. Turland
K. A. Moore

Atomic Energy Establishment (5)
Winfritn, Dorchester
Dorset
England
Attn: R. V. Macbeth
R. Potter
G. L. Shires
G. F. Stevens
R. Trenberth

Culham Laboratory
Culham
Abingdon
Oxfordshire OX14 3DB
England
Attn: F. Briscoe

DISTRIBUTION (continued)

Kernforschungszentrum Karlsruhe (8)
D-75 Karlsruhe
Postfach 3640
West Germany
Attn: G. Heusener (PSB)
P. Hoffmann (PSB)
H. Werle (INR)
L. Barleon (IRB)
G. Hoffman (IRM)
K. Thomauski (IRB)
U. Muller (IRM)
G. Fieg (INR)

University of California (2)
Energy and Kinetics Department
Bolter Hall, Room 5405
Los Angeles, CA 90024
Attn: I. Catton
V. K. Dhir

Argonne National Laboratory (5)
Reactor Analysis and Safety Division
9700 South Cass Avenue
Argonne, IL 60439
Attn: L. Baker, Jr.
J. C. Cassulo
J. D. Gabor
R. D. Pedersen
E. S. Sowa

Westinghouse Electric Corp.
Power Systems
P. O. Box 355
Pitsburgh, PA 15230
Attn: L. Hochreiter

Westinghouse Research and
Development Center
Pitsburgh, PA 15235
Attn: A. Pieczynski

Westinghouse Hanford (2)
337 Bldg., 300 Area
P. O. Box 1970
Richland, WA 99352
Attn: G. R. Armstrong
C. P. Cannon

DISTRIBUTION (continued)

Nuclear Safety Analysis Center (2)
3412 Hillview Avenue
P. O. Box 10412
Palo Alto, CA 94303
Attn: D. Squarer
G. Thomas

Fauske and Associates (2)
631 Executive Drive
Willowbrook, IL 60521
Attn: M. Epstein
R. Henry

Brookhaven National Laboratory (2)
Fast Reactor Safety
Upton, Long Island, NY 11973
Attn: J. W. Yang
T. Ginsberg

Los Alamos National Laboratory
Q7, Slot K556
Los Alamos, NM 87545
Attn: Javier Escamilla

NUS Corporation
Consulting Division
4 Research Place
Rockville, MD 20850
Attn: Juan M. Nieto

EG&G, Idaho (6)
P. O. Box 1625
Idaho Falls, ID 83415
Attn: C. Allison
T. M. Howe
T. S. Hsieh
R. J. Lloyd
R. W. Miller
B. J. Buescher

Massachusetts Institute of Technology (2)
Mechanical Engineering Department
Cambridge, MA 02139
Attn: P. Griffith
M. Kazimi

DISTRIBUTION (continued)

University of New Mexico
Nuclear Engineering Department
Albuquerque, NM 87131
Attn: M. El-Genk

University of Wisconsin (2)
Department of Nuclear Engineering
Madison, WI 53706
Attn: M. Corradini
S. Abdel-Khalik

Purdue University
Department of Nuclear Engineering
West Lafayette, IN 47907
Attn: T. Theofanous

Sandia National Laboratories:
1652 G. W. Mitchell (2)
1271 R. J. Lipinski
1523 R. C. Reuter
1846 R. K. Quinn
3141 C. M. Ostrander (5)
3151 W. L. Garner
6322 C. A. Ottinger (9)
6400 A. W. Snyder
6410 J. W. Hickman
6420 J. V. Walker
6420 M. Hasti
6420 M. Watkins
6421 T. R. Schmidt (5)
6422 D. A. Powers
6423 P. S. Pickard
6423 A. Furutani
6423 G. Schumacher
6425 W. J. Camp
6425 J. E. Kelly (5)
6425 A. W. Reed
6427 M. Berman
6427 J. T. Hitchcock
6430 N. Ortiz
6440 D. A. Dahlgren
6450 J. A. Reuscher
6451 T. F. Luera
6452 M. F. Aker, Jr.
6454 G. L. Cano
8024 M. A. Pound

NRC FORM 335 (2-84) NRCM 1102, 3201, 3202

U.S. NUCLEAR REGULATORY COMMISSION

BIBLIOGRAPHIC DATA SHEET

SEE INSTRUCTIONS ON THE REVERSE

1 REPORT NUMBER (Assigned by TIDC and Vol. No., if any)

NUREG/CR-3757
SAND84-1838

2 TITLE AND SUBTITLE

The D9 Experiment: Heat Removal from Stratified UO_2 Debris

3 LEAVE BLANK

4 DATE REPORT COMPLETED

MONTH	YEAR
February	1985

5 AUTHOR(S)

C. A. Ottinger, G. W. Mitchell,
R. J. Lipinski, J. E. Kelly

6 DATE REPORT ISSUED

MONTH	YEAR
April	1985

7 PERFORMING ORGANIZATION NAME AND MAILING ADDRESS (Include Zip Code)

Degraded Core Coolability Studies
Division 6421
Sandia National Laboratories
Albuquerque, New Mexico 87185

8 PROJECT TASK WORK UNIT NUMBER

9 FIN OR GRANT NUMBER

NRC FIN No.A1181

10 SPONSORING ORGANIZATION NAME AND MAILING ADDRESS (Include Zip Code)

Division of Accident Evaluation
Office of Nuclear Regulatory Research
United States Nuclear Regulatory Commission
Washington, DC 20555

11a TYPE OF REPORT

technical

b PERIOD COVERED (Inclusive dates)

12 SUPPLEMENTARY NOTES

13 ABSTRACT (200 words or less)

The D9 experiment investigated the coolability of a shallow (77 mm), stratified urania bed in sodium. The bed was fission heated in the Annular Core Research Reactor (ACRR) at Sandia National Laboratories to simulate the effects of radioactive decay heating. It was the first stratified debris bed experiment to use an extended UO_2 particle size distribution (0.038 to 4.0 mm). Dryout occurred at powers ranging from 0.10 to 0.58 W/g, which was close to the incipient boiling power and before channels penetrated the subcooled zone in the bed, even with subcoolings as low as 80°C. Channel penetration was observed after dryout began, but the bed became only moderately more coolable. All these observations agree with current models.

14 DOCUMENT ANALYSIS - a KEYWORDS/DESCRIPTORS

b IDENTIFIERS/OPEN ENDED TERMS

15 AVAILABILITY STATEMENT

unlimited

16 SECURITY CLASSIFICATION

(This page)
U

(This report)
U

17 NUMBER OF PAGES

65

18 PRICE

Org.	Bldg.	Name	Rec'd by	Org.	Bldg.	Name	Rec'd by

Sandia National Laboratories